Article

Cell Chemical Biology

Dual-Targeting Small-Molecule Inhibitors of the *Staphylococcus aureus* FMN Riboswitch Disrupt Riboflavin Homeostasis in an Infectious Setting

Graphical Abstract

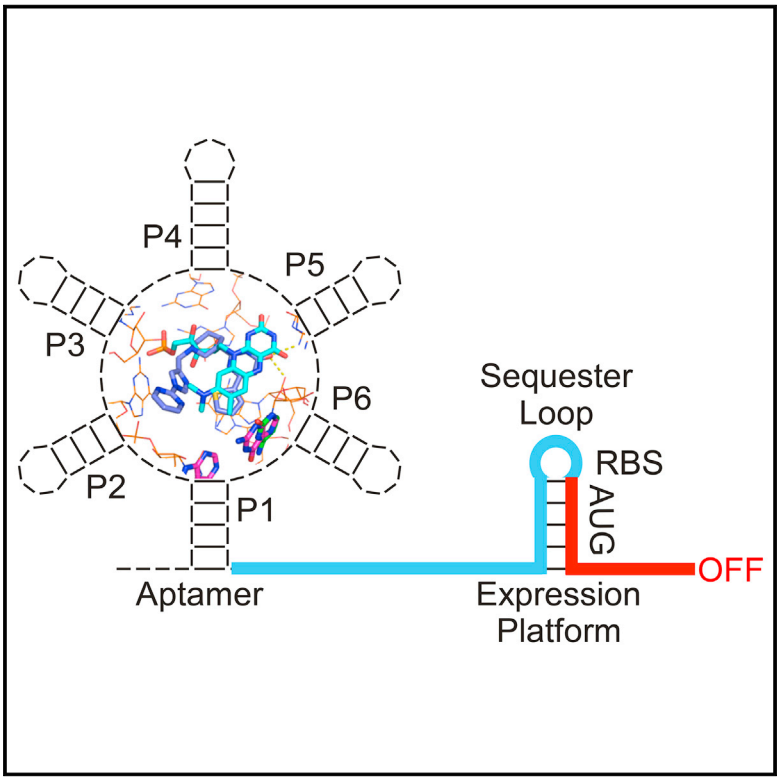

Authors

Hao Wang, Paul A. Mann, Li Xiao, ..., Amy Flattery, Matthias Mack, Terry Roemer

Correspondence

terry_roemer@merck.com

In Brief

Wang et al. demonstrate that ribocil-C and roseoflavin selectively target functionally related non-coding RNA structural elements termed FMN riboswitches controlling gene expression of riboflavin biosynthesis and uptake. Such targets and cognate inhibitors offer new opportunities and challenges to antibiotic discovery.

Highlights

- Ribocil-C and roseoflavin selectively target bacterial non-coding RNA elements
- Each agent inhibits two distinct FMN riboswitches controlling riboflavin metabolism
- Their mechanism is conserved in *Staphylococcus aureus* and *Enterococcus faecalis*
- Dual targeting of FMN riboswitches offer novel antibiotic discovery opportunities

Data Resources

CP019512

Wang et al., 2017, Cell Chemical Biology *24*, 576–588
May 18, 2017 © 2017 Elsevier Ltd.
http://dx.doi.org/10.1016/j.chembiol.2017.03.014

CellPress

CellPress

Cell Chemical Biology
Article

Dual-Targeting Small-Molecule Inhibitors of the *Staphylococcus aureus* FMN Riboswitch Disrupt Riboflavin Homeostasis in an Infectious Setting

Hao Wang,[1] Paul A. Mann,[1] Li Xiao,[1] Charles Gill,[1] Andrew M. Galgoci,[1] John A. Howe,[1] Artjohn Villafania,[1] Christopher M. Barbieri,[1] Juliana C. Malinverni,[1] Xinwei Sher,[1] Todd Mayhood,[1] Megan D. McCurry,[1] Nicholas Murgolo,[1] Amy Flattery,[1] Matthias Mack,[2] and Terry Roemer[1,3,*]

[1]Merck Research Laboratories, Kenilworth, NJ 07033, USA

[2]Department of Biotechnology, Institute for Technical Microbiology, Hochschule Mannheim, Mannheim 68163, Germany

[3]Lead Contact

*Correspondence: terry_roemer@merck.com

http://dx.doi.org/10.1016/j.chembiol.2017.03.014

SUMMARY

Riboswitches are bacterial-specific, broadly conserved, non-coding RNA structural elements that control gene expression of numerous metabolic pathways and transport functions essential for cell growth. As such, riboswitch inhibitors represent a new class of potential antibacterial agents. Recently, we identified ribocil-C, a highly selective inhibitor of the flavin mononucleotide (FMN) riboswitch that controls expression of de novo riboflavin (RF, vitamin B2) biosynthesis in *Escherichia coli*. Here, we provide a mechanistic characterization of the antibacterial effects of ribocil-C as well as of roseoflavin (RoF), an antimetabolite analog of RF, among medically significant Gram-positive bacteria, including methicillin-resistant *Staphylococcus aureus* (MRSA) and *Enterococcus faecalis*. We provide genetic, biophysical, computational, biochemical, and pharmacological evidence that ribocil-C and RoF specifically inhibit dual FMN riboswitches, separately controlling RF biosynthesis and uptake processes essential for MRSA growth and pathogenesis. Such a dual-targeting mechanism is specifically required to develop broad-spectrum Gram-positive antibacterial agents targeting RF metabolism.

INTRODUCTION

Bacterial riboswitches are *cis* regulatory RNA structural elements embedded in untranslated regions (UTRs) of mRNAs that specifically bind natural ligands to regulate gene expression (Winkler et al., 2002; Mironov et al., 2002; Mellin and Cossart, 2015; Winkler and Breaker, 2005). Riboswitches consist of two functionally distinct modules; an aptamer ligand binding domain and a downstream regulatory expression platform (Mellin and Cossart, 2015; Winkler and Breaker, 2005). Mechanistically, binding of the cognate ligand to the aptamer domain induces a conformational change in the expression platform that regulates gene expression typically through attenuation of transcription or inhibition of translation. Riboswitches are thought to regulate the expression of between 1% and 4% of all bacterial genes, and to date more than 35 different classes of riboswitches responding to a diverse set of metabolites have been identified, including enzymatic co-factors such as flavin mononucleotide (FMN) and thiamine pyrophosphate, amino acids such as glycine, lysine, and glutamine, the purines adenine and guanine, and inorganic ions such as magnesium and fluoride (Winkler et al., 2002; Mironov et al., 2002; Serganov and Nudler, 2013; Mack et al., 1998; Winkler and Breaker, 2005; Sudarsan et al., 2005; Breaker, 2011; Baker et al., 2012; Lünse et al., 2014; Mellin and Cossart, 2015).

In bacteria, riboflavin (RF) homeostasis is regulated by FMN riboswitches, one of the most widely distributed classes of RNA regulatory elements (Gutiérrez-Preciado et al., 2015) controlling expression of genes required for biosynthesis and transport of this essential vitamin (Winkler et al., 2002; Mack et al., 1998; Gelfand et al., 1999; Vitreschak et al., 2002; Serganov et al., 2009; Pedrolli et al., 2015a). Starting with guanosine triphosphate and two molecules of ribulose-5-phosphate (Figure S1), RF is synthesized de novo by essentially all bacteria, yeasts, and plants (Fischer and Bacher, 2005). Conversely, vertebrates lack enzymes required to synthesize RF and instead acquire the vitamin exclusively from their diet. Importantly, RF serves as the immediate precursor of FMN and flavin adenine dinucleotide (FAD), two critical co-factors to a ubiquitous family of flavoenzymes that play essential redox reactions in diverse aspects of cellular metabolism (Fischer and Bacher, 2005). FMN serves as the primary regulatory ligand of FMN riboswitches and, although RF and FAD can also associate with the FMN riboswitch aptamer, their affinity is low and they do not play an important role in gene regulation (Mack et al., 1998; Winkler et al., 2002; Lee et al., 2009; Serganov et al., 2009). Mechanistically, FMN binding to its cognate riboswitch induces a conformational change within the expression platform (hence referred to as a "riboswitch") that obscures a ribosome binding sequence (RBS) within the expression platform, thus reducing expression of *rib* genes under the control of the FMN riboswitch and involved in RF biosynthesis or active transport (Figure 1) (Winkler et al., 2002; Mironov et al., 2002; Vitreschak et al., 2002; Serganov et al., 2009; Pedrolli et al., 2015a). Conversely, when FMN cellular levels are low and the

CrossMark

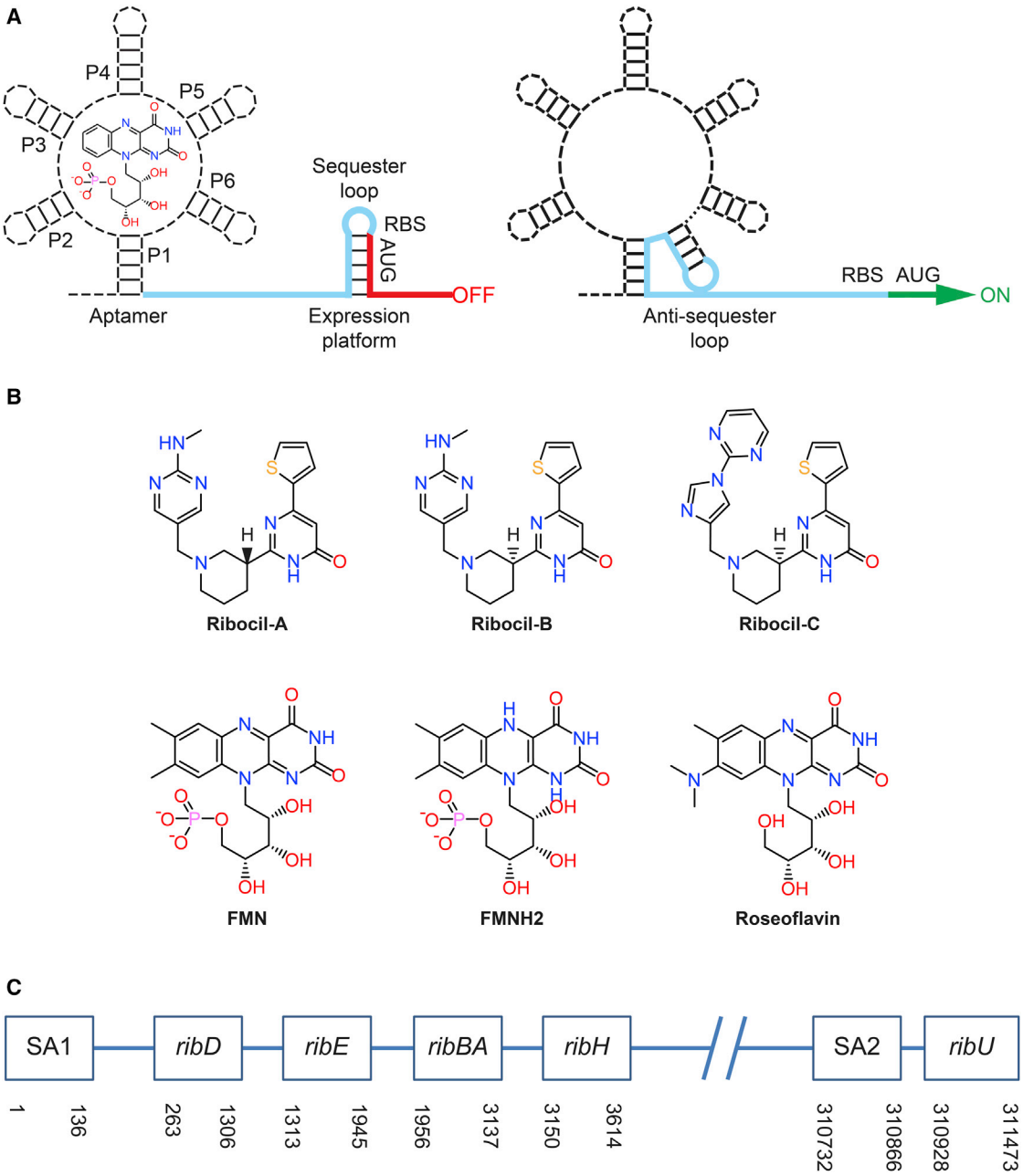

Figure 1. FMN Riboswitch Regulation, Cognate Inhibitors, and RF Homeostasis Gene Organization

(A) Schematic structure of the FMN riboswitch containing the 5′ mRNA FMN aptamer that binds FMN and the 3′ expression platform (blue) that directly coordinates expression of the downstream *rib* open reading frame. Left, FMN aptamer binding to the FMN ligand transduces a conformational change in the expression platform (OFF), resulting in the formation of a terminator/sequester loop that abolishes *rib* expression by sequestering the RBS to prevent translation of completely transcribed *rib* mRNAs. Right, when FMN levels are low, the FMN aptamer lacking the bound ligand adopts a second structural conformation (ON) that induces an anti-terminator/anti-sequester loop, thereby facilitating uninterrupted *rib* expression.

(B) Chemical structure of ribocil-A, ribocil-B, ribocil-C, FMN, FMNH2, and roseoflavin.

(C) Gene organization of MRSA COL RF biosynthetic operon and *ribU* transporter, with relative genome coordinates from GB accession CP000046.1. FMN riboswitches SA1 and SA2 regulate the RF biosynthetic operon and *ribU* RF transporter, respectively. See also Figure S1.

regulatory ligand is unbound to the aptamer, the riboswitch adopts an alternative structural conformation that exposes the RBS within the expression platform to facilitate *rib* gene expression (Figure 1) (Winkler et al., 2002; Mironov et al., 2002; Vitreschak et al., 2002; Serganov et al., 2009; Pedrolli et al., 2015a). Consequently, the FMN riboswitch serves as a finely tuned post transcriptional (and in some instances transcriptional; Pedrolli et al., 2015a) negative regulatory circuit to coordinate RF synthesis and uptake according to FMN cellular levels.

Considering the essential role of FMN riboswitch-mediated gene regulation in bacterial physiology, its broad conservation within the FMN ligand binding domain to accommodate a common regulatory metabolite, and the absence of an orthologous gene regulation system in humans, it has recently been considered a potential broad-spectrum antibacterial drug target (Blount and Breaker, 2006; Ott et al., 2009; Mulhbacher et al., 2010; Pedrolli et al., 2013; Lünse et al., 2014; Matzner and Mayer, 2015). However, its potential spectrum as a suitable drug target must address the functional dichotomy and redundancy of FMN riboswitches involved in RF homeostasis between Gram-negative (GN) and Gram-positive (GP) bacterial pathogens. Specifically, GN bacteria are broadly dependent on a single FMN riboswitch to control de novo biosynthesis of the vitamin as they lack an active transport mechanism to scavenge external sources of RF (Gutiérrez-Preciado et al., 2015). Conversely, GP pathogens including *Enterococcus faecalis* and *Streptococcus pyogenes* are RF auxotrophs, lacking the *rib* RF biosynthetic operon and are entirely dependent on a single FMN riboswitch controlling expression of the RF transporter to scavenge RF within an infectious setting (Gutiérrez-Preciado et al., 2015). Finally, other GP bacterial pathogens such as *Staphylococcus aureus* efficiently obtain RF either from the host environment or, when exogenous sources are insufficient, rely on de novo RF biosynthesis (Zhang et al., 2010; Gutiérrez-Preciado et al., 2015). Indeed expression of the RF transporter, encoded by *ribU* as well as the entire *rib* RF biosynthetic operon are both under the control of highly related FMN riboswitches (Figure 1) (Gutiérrez-Preciado et al., 2015). Therefore, substantial genetic and pharmacological validation studies remain to be performed both in vitro as well as in a host infection environment to warrant FMN riboswitches being viewed as suitable broad-spectrum antibacterial targets and to demonstrate that their inhibition is not suppressed by endogenous RF levels in a host setting, analogous to the fatty acid synthase antibacterial drug target and its species-dependent suppression by host fatty acids (Brinster et al., 2009; Morvan et al., 2016).

Roseoflavin (RoF; Figure 1) is a natural product analog of RF originally isolated from *Streptomyces davawensis* (Otani et al., 1974), which inhibits growth of *Bacillus subtilis*, *Escherichia coli*, and *Listeria monocytogenes* by targeting FMN riboswitches (Lee et al., 2009; Serganov et al., 2009; Ott et al., 2009; Mansjo and Johansson, 2011; Pedrolli et al., 2012, 2015a, 2015b). RoF is a prodrug which is sequentially converted to roseoflavin mononucleotide (RoFMN) and roseoflavin adenine dinucleotide (RoFAD) by essential flavokinase and synthetase enzymes, respectively (Ott et al., 2009). Interestingly, as an analog of RF, RoF is actively transported into GP bacteria by RF transporters prior to its conversion to RoFMN and subsequent repression of FMN riboswitch-mediated RF gene expression and ultimate growth inhibition (Mansjo and Johansson, 2011; Gutiérrez-Preciado et al., 2015; Pedrolli et al., 2015a).

Recently, we reported the discovery of ribocil-C (Figure 1), a small-molecule synthetic mimic of FMN that binds the FMN riboswitch of multiple GN bacteria, including *E. coli*, *Pseudomonas aeruginosa*, and *Acinetobacter baumannii*, to inhibit *ribB* expression, RF synthesis, and consequently arrest bacterial growth (Howe et al., 2015, 2016). Here we broadly investigate the mechanism of action (MOA) of ribocil-C and RoF in inhibiting GP bacterial pathogens, with particular emphasis on methicillin-resistant *S. aureus* (MRSA) and *E. faecalis*. We demonstrate ribocil-C and RoF are highly specific GP FMN riboswitch inhibitors and apply these agents as chemical probes to demonstrate their dual-targeting mechanism of interdicting *S. aureus* FMN riboswitches is uniquely required to develop broad-spectrum GP antibacterial agents targeting RF metabolism.

RESULTS

Microbiological Activity of Ribocil and RoF against GP Bacteria

Ribocil is synthesized as a racemic mixture of ribocil-A (R-isomer) and ribocil-B (S-isomer) enantiomers, with ribocil-B solely responsible for *E. coli* antibacterial activity and its analog ribocil-C displaying superior potency (Figure 1) (Howe et al., 2015, 2016). Based on their highly selective mechanism of inhibiting GN FMN riboswitches, we evaluated the potential expanded antibacterial spectrum of ribocil-A-C as well as RoF against clinically relevant GP bacteria including *S. aureus*, *E. faecalis*, and *S. pyogenes* tested under a variety of RF supplementation growth conditions. Determining their minimum inhibitory concentration (MIC) when tested in cation-adjusted Mueller Hinton broth (CAMHB) medium containing trace RF levels, ribocil-C displayed robust growth-inhibitory activity against MRSA COL as well as the methicillin-sensitive *S. aureus* isolate, RN4220 (MIC = 0.5 μg/mL) versus intermediate ribocil-B activity (MIC = 4 μg/mL) and ribocil-A which lacked anti-Staphylococcal activity, paralleling their relative *E. coli* activity (Table 1) (Howe et al., 2015). RoF displayed superior activity (MIC = 0.063 μg/mL) against each isolate. RoF also exhibits superior activity against *E. faecalis*, and *S. pyogenes* growth (MIC = 0.063–1 μg/mL) versus ribocil-C (MIC = 8–32 μg/mL). Notably, all agents displayed substantially reduced GP antibacterial activity when tested with increasing concentrations of RF supplemented into CAMHB medium (Table 1). Ribocil-C and RoF also both appear to demonstrate high selectivity toward *S. aureus* FMN riboswitches as ribocil-C activity was completely suppressed by 0.2 μM RF addition, and RoF activity was also suppressed albeit at a 10-fold higher RF concentration (Figure S2). Consistent with this view, ribocil-B and ribocil-C strongly inhibit FMN synthesis in MRSA COL, with half maximal inhibitory concentration (IC_{50}) values of 0.44 and 0.05 μM, respectively, paralleling their previously reported relative activity against *E. coli* (Figure 2A) (Howe et al., 2015).

Previously, we demonstrated that *E. coli* strains deleted of *ribA*- or *ribB*-mediated RF biosynthesis are avirulent and that ribocil-C provides a dose-dependent efficacy against an RF biosynthetic-competent *E. coli* strain in a murine infection model (Howe et al., 2015). These data provide compelling genetic and pharmacological evidence that RF biosynthesis is a valid antibacterial target, the inactivation of which is not suppressed by RF in an infectious setting, presumably because GN bacteria lack an active transport system for RF uptake. Alternatively, dramatic RF-based suppression of RoF and ribocil-C in vitro antibacterial activity against *S. aureus* and other GP bacteria suggest that ubiquitously expressed GP RF transporters

Table 1. Ribocil-C and RoF Antibiotic Activity against Gram-Positive Bacteria

	Ribocil	Ribocil-A	Ribocil-B	Ribocil-C	RoF	Linezolid
MIC in CAMHB (μg/mL)						
MSSA RN4220	8	>64	4	0.5	0.06	1
MRSA COL	8	>64	4	0.5	0.06	1
MRSA COL Δ*ribD*	NG	NG	NG	NG	NG	NG
E. faecalis	NG	NG	NG	NG	NG	NG
S. pyogenes[a]	>64	>64	>64	8	0.06	0.5
MIC in CAMHB +12.5 nM RF (μg/mL)						
MSSA RN4220	>64	>64	>64	>64	0.5	1
MRSA COL	>64	>64	>64	>64	0.5	1
MRSA COL Δ*ribD*	>64	>64	>64	>64	0.5	1
E. faecalis	>64	>64	>64	32	1	8
S. pyogenes[a]	>64	>64	>64	>64	0.5	0.5
MIC in CAMHB +200 nM RF (μg/mL)						
MSSA RN4220	ND	ND	ND	ND	8	1
MRSA COL	ND	ND	ND	ND	16	1
MRSA COL Δ*ribD*	ND	ND	ND	ND	8	1
E. faecalis	ND	ND	ND	ND	4	8
S. pyogenes[a]	ND	ND	ND	ND	8	0.5
MIC in CAMHB +50% human serum (μg/mL)						
MSSA RN4220	ND	ND	ND	ND	4	1
MRSA COL	ND	ND	ND	ND	4	1
MRSA COL Δ*ribD*	ND	ND	ND	ND	4	1
E. faecalis	ND	ND	ND	ND	8	8
S. pyogenes	ND	ND	ND	ND	64	0.5
IC_{50} of FMN biosynthesis (μM)						
MRSA COL	ND	>10	0.44	0.04	0.04	ND
MRSA COL WTM6 (SA1)	ND	ND	ND	4.6	11.2	ND
MRSA COL WTM22 (Azo1)	ND	ND	ND	0.08	>40	ND

NG, no growth; ND, not determined.
See also Figures S2 and S6.
[a]Supplemented with 5% lysed horse blood.

(Gelfand et al., 1999; Vogl et al., 2007; Zhang et al., 2010; Gutiérrez-Preciado et al., 2015) could potentially jeopardize their efficacy in an infectious setting. Consistent with this possibility, 100-fold lower RF levels were required to fully suppress ribocil-C activity against MRSA COL than *E. coli* (Figure S2). We also constructed an *E. coli* strain heterologously expressing the *pnuX* RF transporter from *Corynebacterium glutamicum* (Vogl et al., 2007) and compared its susceptibility with ribocil-C versus the isogenic parent strain lacking an RF transport system. Ribocil-C activity against this *E. coli* RF transporter competent strain was similarly suppressed with 100-fold lower levels of RF, resembling the highly efficient RF-specific suppression of ribocil-C and RoF activity against *S. aureus* (Figure S2). We also observed that the *E. coli pnuX*-expressing strain displayed increased sensitivity to RoF, consistent with its high structural similarity to RF and substrate of RF transporters (Vogl et al., 2007). Conversely, as the *E. coli pnuX*-expressing strain demonstrated no change in ribocil-C susceptibility versus the vector control, we conclude ribocil-C is not a substrate of RF transporters. Collectively, these data suggest that novel FMN riboswitch inhibitors need not enter GP bacteria via RF transporters and, importantly, the antibacterial efficacy of such agents is likely dependent on endogenous RF levels in an infectious setting.

Ribocil-C Specifically Binds *S. aureus* FMN Riboswitches Controlling RF De Novo Synthesis and Uptake

RF suppression data imply that the MOA of ribocil-C is conserved between *E. coli* and *S. aureus*. To demonstrate this directly, we first assessed by biophysical means its relative affinity to distinct *S. aureus* FMN riboswitches regulating the RF biosynthetic operon (SA1) and the RF transporter, *ribU* (SA2). SA1 and SA2 aptamers are highly related to one another (96% identity; Figure S3). Synthetic SA1 and SA2 FMN aptamers were purified and their structural integrity confirmed for FMN binding using a previously described fluorescence-quenching assay (Howe et al., 2015) (Figure 2B). Addition of ribocil-C directly competed with FMN binding to both FMN aptamers in vitro in a potent and dose-dependent manner (Figure 2C).

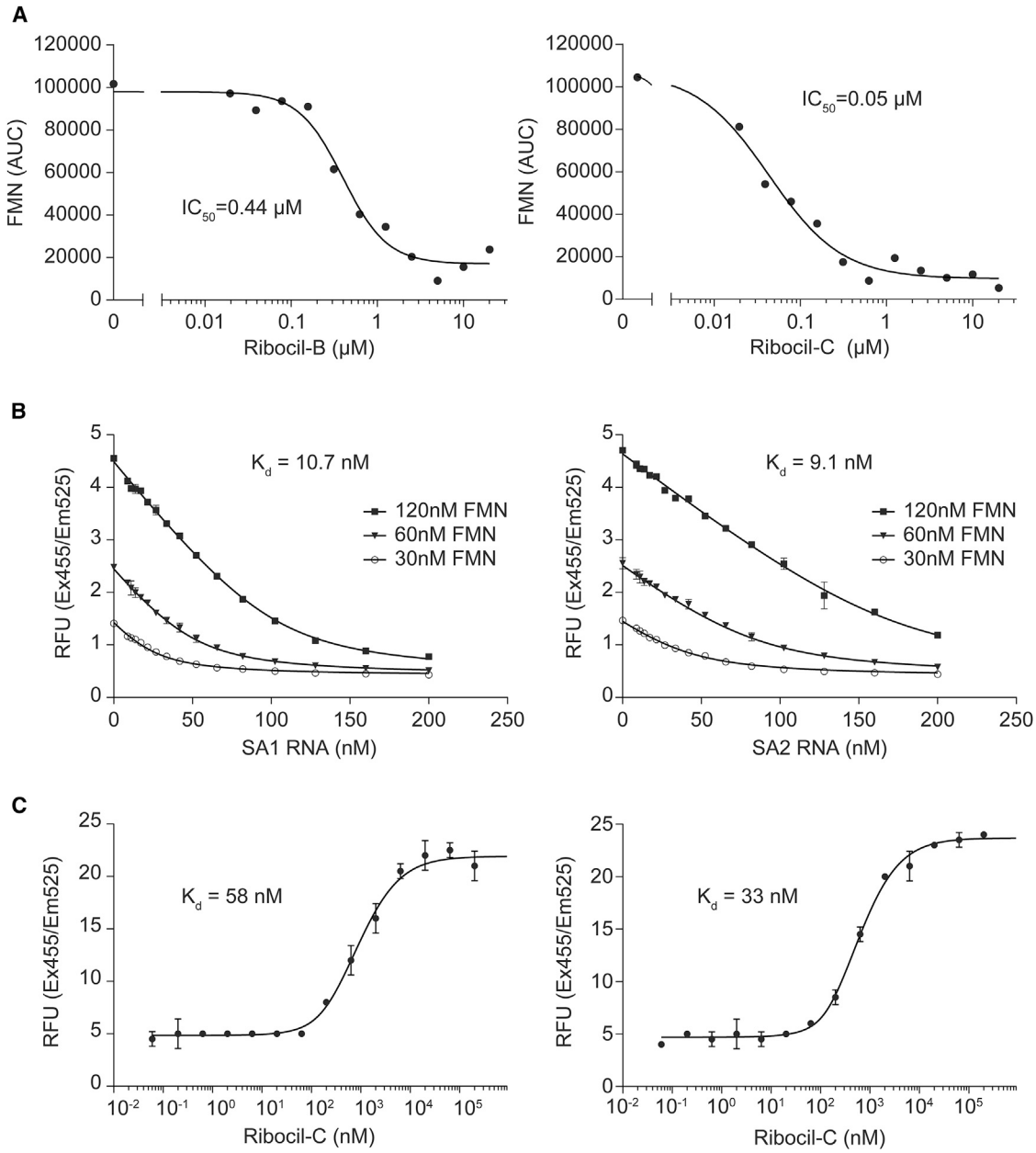

Figure 2. Ribocil-C and FMN Binding Affinity to *S. aureus* SA1 and SA2 FMN Riboswitch Aptamers

(A) HPLC analysis of dose-response inhibition of cellular FMN synthesis in MRSA COL by ribocil-B and ribocil-C (AUC, area under the curve). The median inhibitory concentration (IC_{50}) of ribocil-B and ribocil-C are 0.44 and 0.05 μM, respectively.

(B) FMN binding affinity to SA1 (left) and SA2 (right) is determined from riboswitch aptamer-dose-dependent changes in FMN fluorescence signal. The solid lines represent the non-linear least-squares analysis of the data as described in the methods. This analysis also yields the binding-competent fraction of riboswitch aptamer, 1.16 and 0.68 for SA1 and SA2, respectively.

(C) Ribocil-C binding affinity to the SA1 (left) and SA2 (right) FMN riboswitch aptamers is determined from ribocil-C dose-dependent competition against a fixed concentration of FMN (60 nM) and a fixed concentration of the corresponding riboswitch aptamer (150 nM). The solid lines represent the non-linear least-squares analysis of the data as described in the methods.

Further, ribocil-C demonstrated similar binding affinities to SA1 and SA2 aptamers, with determined K_d values of 58 and 33 nM, respectively. FMN, the natural riboswitch ligand, binds SA1 and SA2 aptamers with only slightly greater affinities (10.7 and 9.1 nM, respectively) versus the synthetic mimic, ribocil-C (Figure 2B).

Homology Modeling of Ribocil-C and RoF Binding into Highly Conserved *S. aureus* and *E. coli* FMN Riboswitch Aptamer Domains

To provide a molecular-level understanding of ribocil-C and RoF binding to *S. aureus* SA1 and SA2 versus the *E. coli* FMN riboswitch, we built homology models for SA1, SA2, and the *E. coli*

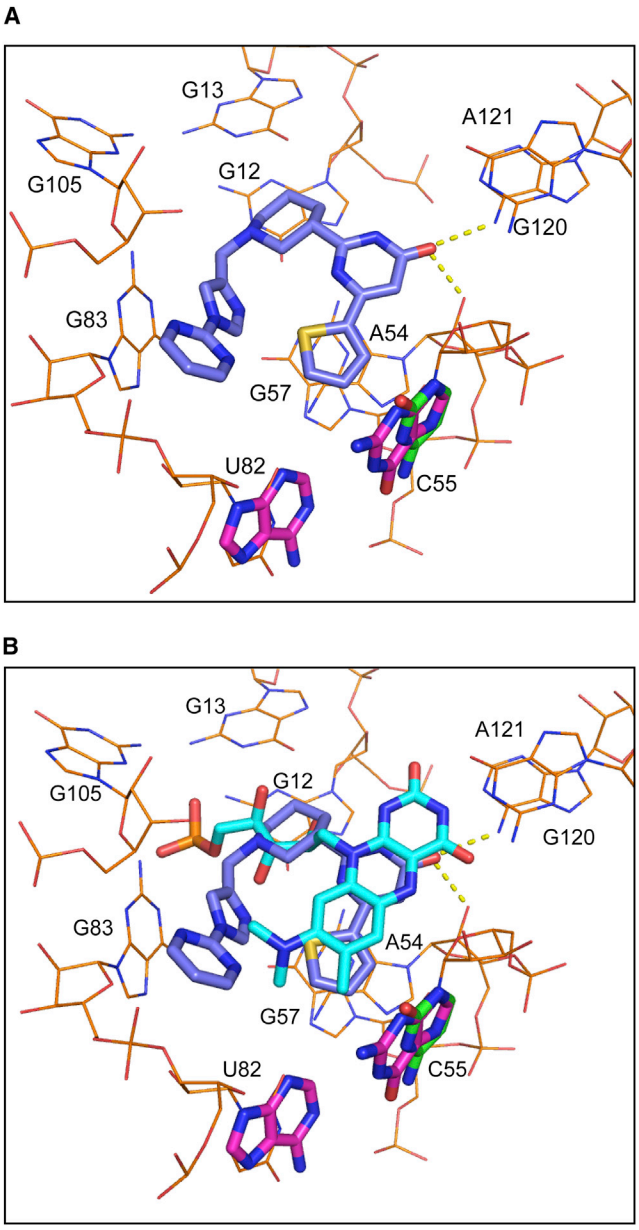

Figure 3. Comparison of *S. aureus* SA1, SA2, and *E. coli* FMN Riboswitch Ligand Binding Sites

(A) Ribocil-C binding site in *S. aureus* SA1 FMN riboswitch. Ribocil-C carbon atoms in light blue. Nucleic acid changes are highlighted in stick, single change C55 of SA1 and SA2 in green, two variants C55/G, U82/A of *E. coli* highlighted in magenta. A106 was removed for clarity.

(B) Structural superposition of ribocil-C and RoFMN. RoFMN carbon atoms in cyan.

FMN riboswitch aptamer using X-ray structures of the *Fusobacterium nucleatum* FMN riboswitch in complex with ribocil-C and RoF (Serganov et al., 2009; Howe et al., 2015). Ribocil-C was modeled using the ribocil-B X-ray structure and displays a very similar binding mode as ribocil-C (Howe et al., 2016). Structural overlay of the FMN riboswitch aptamer models reveals that within 5 Å radius of the ligands, most of the binding site nucleic acids are conserved, except nucleic acids C55 and U82 of SA1 and SA2 (Figure 3). The C55 position is a G in the consensus sequence derived from more than 180 FMN riboswitch sequences of various species, including *E. coli* FMN riboswitch (RFAM database), whereas U82 changes to an A in the consensus sequence as well as in *E. coli*. These changes, C55/G and U82/A, as in both SA1 and SA2 versus the *E. coli* FMN riboswitch, respectively, are bound to the thiophene group of ribocil-C and the tricyclic core of RoF, where mainly aromatic stacking and hydrophobic interactions are involved in ligand binding. Thus these nucleic acid changes are not expected to significantly affect binding activity as the varied bases should maintain similar aromatic interactions with the ligands. Combined with the fact that regions where there are H-bond interactions between these ligands and the FMN riboswitch is broadly conserved, the molecular model of the structures of *S. aureus* SA1, SA2, and *E. coli* FMN riboswitches provide a clear molecular basis for the similarly high binding potency of ribocil-C and RoF to the FMN riboswitch among these bacteria.

Genetic Analysis of Ribocil-C and RoF MOA

Drug-resistant selection and whole-genome sequencing (WGS) was performed in MRSA COL to directly determine the MOA of RoF and ribocil-C in a whole-cell context. As ribocil-C does not completely inhibit MRSA growth on agar plates (thus precluding direct resistant mutant isolation), RoF resistant (^{R}) MRSA isolates were first characterized and cross-resistance to ribocil-C subsequently assessed. Thirty-one MRSA RoF^R mutants were isolated and drug^R mutants mapped by WGS (Figure S4A). Twenty-nine RoF^R resistors contain a single base substitution in their genome, with each mutation faithfully mapping to the SA1 riboswitch controlling expression of the RF biosynthetic operon (Figures 4A and S4A). RoF resistors comprise 11 distinct SA1 FMN riboswitch genotypes, each located specifically within the FMN aptamer rather than the expression platform element (Figure 4A). As no additional mutations were identified in any of the sequenced genomes of the RoF^R isolates, we conclude each of these mutations is causal for RoF^R (Table S1). Interestingly, two additional independently derived RoF^R isolates contain a single missense mutation, P139S (WTM15) and S124L (WTM22) (Figure S4A), mapping to Azo1, a previously characterized FMN reductase not known to confer RoF resistance or provide any functionally demonstrated role in RF metabolism or flavoenzyme co-factor synthesis (Chen et al., 2005) (see Discussion). Cross-resistance studies demonstrate all 11 distinct RoF^R SA1 FMN riboswitch mutants also display high level resistance to ribocil-C, with MIC shifts of >32-fold (Table S1). Therefore, ribocil-C also not only binds to the *S. aureus* SA1 FMN aptamer in vitro but functionally inhibits the FMN riboswitch in whole cells. Conversely, whereas Azo1 S124L and P139S RoF^R isolates each displayed a 256-fold change in RoF susceptibility, no noticeable cross-resistance to ribocil-C was observed, indicating an important difference in mechanisms of resistance between the two inhibitors (Table S1).

To further characterize RoF and ribocil-C resistance, FMN and FAD levels were determined among each of the distinct RoF^R mutants isolated versus wild-type MRSA after ribocil-C or RoF treatment (Figure S5). As all RoF^R mutants produce FMN and FAD at no more than 2-fold greater levels than the isogenic

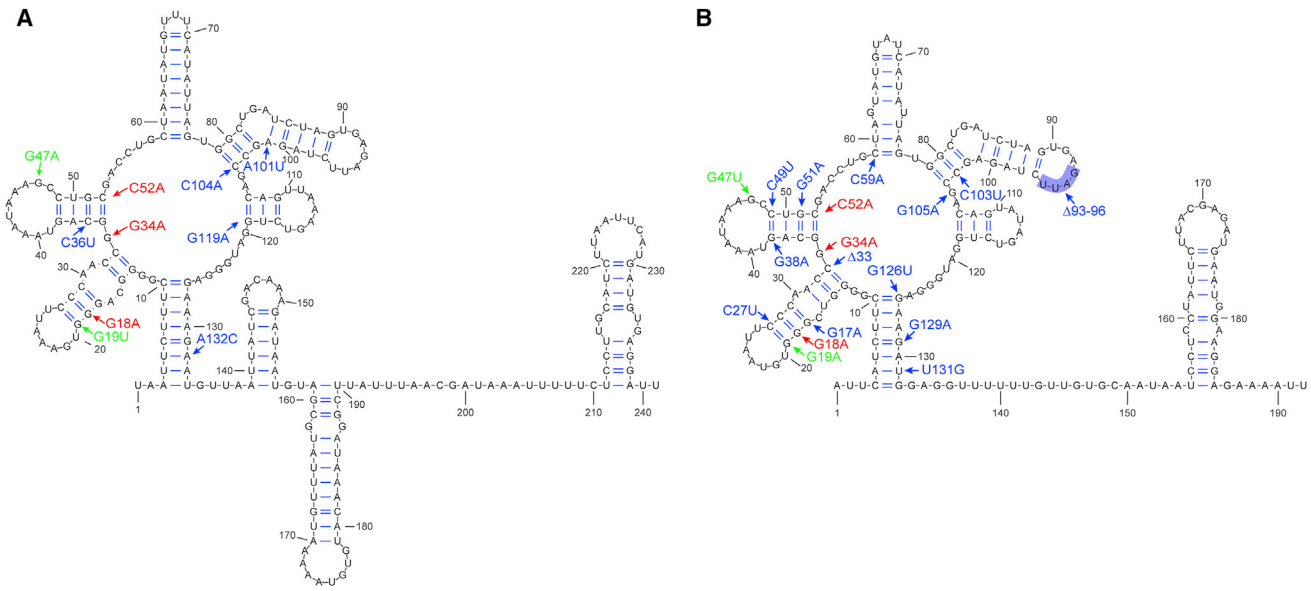

Figure 4. RoF^R Mutation Mapping to *S. aureus* SA1 and SA2 FMN Riboswitches

Predicted secondary structure of the *S. aureus* SA1 and SA2 FMN riboswitches. Independently isolated single-base RoF^R mutations that are common to both SA1 (A) and SA2 (B) FMN riboswitches are indicated in red. RoF^R mutations that occur at homologous bases common to each riboswitch but yielding different substituted bases are indicated in green. RoF^R mutations unique to either SA1 or SA2 FMN riboswitch are indicated in blue. *S. aureus* SA1 and SA2 FMN riboswitch secondary structure predictions were derived following their alignment against a Hidden Markov Model (HMM) of genome scans using the RFAM model RF0050 as downloaded from the RFAM database (Burge et al., 2012). See also Figures S3–S5, S7, and S8; Tables S1 and S2.

wild-type strain, we conclude that ribocil-C resistance is not mediated by mutations conferring a striking upregulation of RF synthesis. Indicative of their cross-resistance, 8 of 11 distinct SA1 RoF^R mutant classes express comparable or greater FMN and FAD levels in ribocil-C-treated cells compared with the detected FMN and FAD levels in wild-type untreated cells. Moreover, RoF^R mutants WTM1 (A132C), WTM6 (A101U), and WTM10 (C36U) also produce greater FMN and/or FAD levels in ribocil-C treated cells than detected in identically drug-treated wild-type cells. We speculate such residual levels of FMN and FAD are likely sufficient for growth.

RoF and ribocil-C resistance were additionally examined in a representative RoF^R mutant mapping to SA1 (WTM6; A101T) and Azo1 (WTM22; S124L) to determine their effects on FMN levels in drug-treated resistor isolates. As predicted, SA1 mutant WTM6 displayed dramatic dose-dependent resistance to ribocil-C and RoF (Table 1). Whereas both agents demonstrate similar IC_{50} values of 0.04 μM against wild-type MRSA, their respective IC_{50} values to inhibit FMN synthesis were 4.6 and 11.2 μM, respectively against RoF^R mutant WTM6. Conversely, RoF^R mutant WTM22 specifically conferred resistance to RoF-mediated inhibition of intracellular FMN levels (IC_{50} > 40 μM) (Table 1). These results demonstrate important distinctions in the drug-resistance mechanisms between ribocil-C and RoF (see below).

RoF and Ribocil-C Are Dual-Targeting Inhibitors of Both SA1 and SA2 FMN Riboswitches in *S. aureus*

Based on in vitro evidence that ribocil-C binds SA1 and SA2 FMN aptamers with affinities approaching that of FMN and that each of the aptamers are highly structurally related, we sought whole-cell evidence demonstrating that ribocil-C and RoF each also target the SA2 FMN riboswitch controlling *ribU* RF transporter expression. To demonstrate this, we first constructed a strain deficient in de novo RF biosynthesis by deletion of *ribD* (the first gene in the *S. aureus* RF biosynthetic operon encoding an RF-specific deaminase and directly regulated by the SA1 FMN riboswitch), thus rendering the Δ*ribD* strain exclusively reliant on SA2-dependent expression of *ribU*. Indeed, the Δ*ribD* strain displays an RF auxotrophy suppressed by exogenously added RF (Figure S6) similar to wild-type *E. faecalis* and *S. pyogenes* strains which are natural RF auxotrophs lacking RF biosynthetic enzymes and solely reliant on FMN riboswitch-regulated RF transporters (Gutiérrez-Preciado et al., 2015). Ribocil-C modestly inhibited growth of the MRSA Δ*ribD* strain as well as *S. pyogenes* and fully inhibited *E. faecalis* growth (Table 1 and Figure S6). RF-mediated suppression of ribocil-C antibacterial activity against all three strains tested (Table 1 and Figure S6) is consistent with the compound inhibiting the FMN riboswitch regulating *ribU*. Similarly, RoF inhibited all three strains with superior potency versus ribocil-C and was suppressed in an RF-dependent manner (Table 1 and Figure S6). Considering that at a fixed drug concentration (20× MIC) measurably more RF is required to suppress RoF activity than ribocil-C activity against both the MRSA wild-type and Δ*ribD* strain, we speculate that RoF is a more potent inhibitor of the SA2 FMN riboswitch than ribocil-C (Figure S6).

To directly demonstrate that RoF and ribocil-C target the SA2 FMN riboswitch in a cellular milieu, we again performed drug^R selection studies. Previous MRSA COL RoF^R selection studies were likely biased to isolating mutants that mapped exclusively to the SA1 riboswitch due to the fact that no exogenous RF

was present during drug selection, and therefore cells were solely dependent on de novo RF biosynthesis. Consequently, neither the SA2-mediated FMN riboswitch nor RibU would have a functional role, thus undermining the likelihood of drug^R mutations mapping to this pathway. Therefore, RoF^R mutant isolation was performed in an MRSA Δ*ribD* strain solely dependent on SA2 FMN riboswitch-mediated RibU RF transport. Under such conditions, 27 stable RoF^R mutants were isolated and, following WGS, each resistor was found to contain a base substitution or deletion that maps specifically to the SA2 aptamer (Figures 4B and S4B), with only three additional resistors isolated containing a nonsynonymous mutation elsewhere in their sequenced genome (Figure S4B). Accordingly, SA2 mutations are causal for RoF^R in this strain background. Indeed, nearly all base substitutions conferring RoF^R are located within common hairpin loops shared between SA1 and SA2 (Figure 4B). Three RoF^R mutants originally selected under conditions that favor the SA1-based resistance are independently isolated and map to SA2 under conditions favoring SA2 resistance selection (Figure 4B). Remarkably, these mutations map to conserved bases shared between SA1 and SA2 aptamers and their base substitutions are identical (G18A, G34A, and C52A). Similarly, two additional RoF^R mutations map to conserved bases within SA1 and SA2 aptamers, differing only in base substitution (G19U/A and G47A/T) (Figure 4). Unexpectedly, RoF MIC shifts between each of these SA2 FMN riboswitch RoF^R mutants in the isogenic Δ*ribD* strain (Table S2) are less pronounced (4- to 8-fold) than observed against SA1 FMN riboswitch RoF^R mutants in the wild-type parent MRSA strain, which exceed 512-fold (Table S1 and see Discussion). As ribocil-C displays poor growth-inhibitory activity against the MRSA Δ*ribD* strain in liquid medium (Table S2), cross-resistance studies were performed by serial dilution and spotting of each of the SA2 FMN riboswitch RoF^R mutants on cation-adjusted Mueller Hinton (CAMH) agar plates supplemented with 12.5 nM RF and 20 μM ribocil-C (Figure S7). Under these assay conditions, substantial cross-resistance between ribocil-C and each SA2 FMN riboswitch RoF^R mutant was observed. Collectively, these data provide compelling genetic evidence that RoF and ribocil-C each possess a multi-target MOA to inhibit *S. aureus* that involves disruption of dual SA1 and SA2 FMN riboswitches required to sustain RF levels sufficient for bacterial growth.

To extend RoF and ribocil-C MOA studies to *E. faecalis*, we again sought to identify target-based drug^R mutations. Four RoF^R mutants were isolated, each yielding an 8- to 16-fold reduced susceptibility to RoF (Figure S8). WGS revealed three separate classes of single mutations in the genome of each resistor. Surprisingly, none of these mutations map to the FMN riboswitch controlling *ribU* expression, perhaps because such mutations could significantly compromise the expression of *ribU* essential to the survival of this natural auxotroph (see Discussion). Instead, one isolate maintains a missense mutation which maps to the *ribU* open reading frame and confers a G80E amino acid substitution within the RF transporter. To the best of our knowledge, this is the first time an RoF^R mutation has been identified within the RF transporter. We speculate that the RoF^R of this mutant may manifest as a reduced affinity of the RF transporter for RoF versus its cognate substrate. Two isolates also contain a single base substitution within an intergenic region 124 bp upstream of an exodeoxyribonuclease III (EF2734) and 64 bp downstream of a Gfo/Idh/MocA family oxidoreductase (EF2735). Although it is tempting to speculate that this intergenic region may contain a novel FMN riboswitch, this region is not conserved in other bacterial species and bioinformatics algorithms fail to predict a riboswitch RNA secondary structure. Finally, one RoF^R isolate maintains a nonsense mutation causing a C-terminal truncation at residue 121 within the uncharacterized flavoenzyme, EF1586, and its basis of drug resistance is unknown.

Dual Inhibition of RF De Novo Synthesis and Uptake Are Required to Demonstrate Efficacy in a Murine Model of MRSA Infection

To investigate the relative importance of de novo RF biosynthesis and active uptake of RF in a relevant infectious setting, we first examined the virulence phenotype of the MRSA Δ*ribD* strain versus MRSA COL in a previously described murine septicemia model of infection (Lee et al., 2016). No significant difference in bacterial burden within spleens of infected mice was detected between the two MRSA strains over a 3 $\log_{10}$ range in infectious doses tested (Figure 5A). As the MRSA Δ*ribD* strain is unable to synthesize RF de novo and its growth is dependent on RF uptake, we conclude that *S. aureus* can effectively scavenge sufficient RF in this infection model. Consistent with this view, the average RF concentration in human plasma reported among over 1,000 patients evaluated is ~18 nmol/L, with a range of 5.5–61 nmol (Petteys and Frank, 2011), a level far higher than required to fulfill a wild-type growth rate of the Δ*ribD* strain under in vitro conditions (Figure S6). In addition, as little as 10% heat-inactivated human serum supplemented in CAMH, a medium in which RF levels are otherwise insufficient for growth of the Δ*ribD* strain, fully rescued growth of the *S. aureus* RF auxotroph (Figure 5B). Similarly, 10% human serum rescued RF auxotrophy of both *E. faecalis* and *S. pyogenes* (Figure 5B). Consistent with these findings, ribocil-C and RoF activity against these three species is dramatically reversed in the presence of serum (Table 1). Thus, each of the GP bacterial pathogens examined effectively scavenges RF under in vivo or ex vivo conditions, which would offset the efficacy of any agent that solely inhibits de novo RF biosynthesis.

Based on the above data, a dual-targeting FMN riboswitch inhibitor such as RoF or ribocil-C that impairs both de novo RF biosynthesis and RibU-mediated RF uptake may uniquely provide efficacy against an *S. aureus* infection. To test this possibility, we evaluated the effects of RoF treatment in a relevant murine septicemia model of infection (Figure 5C). Bacterial burden in sham-treated mice infected with wild-type MRSA or the isogenic Δ*ribD* strain ranged between 7.5 and 8 $\log_{10}$ (colony forming units [CFU] per g spleen) at 24 hr post challenge. However, up to a 2 $\log_{10}$ dose-dependent reduction in bacterial burden of either MRSA strain was reproducibly detected following subcutaneous administration of 50 or 100 mg/kg RoF (Figure 5C). Notably, one animal succumbed to the MRSA Δ*ribD* infection at the 50 mg/kg dose and side effects were observed including lethargy and ruffled fur. Therefore, although RoF likely has inherent off-target toxicity, these data provide a pharmacological demonstration that a more selective and potent dual-targeting FMN riboswitch inhibitor that blocks both RF de novo

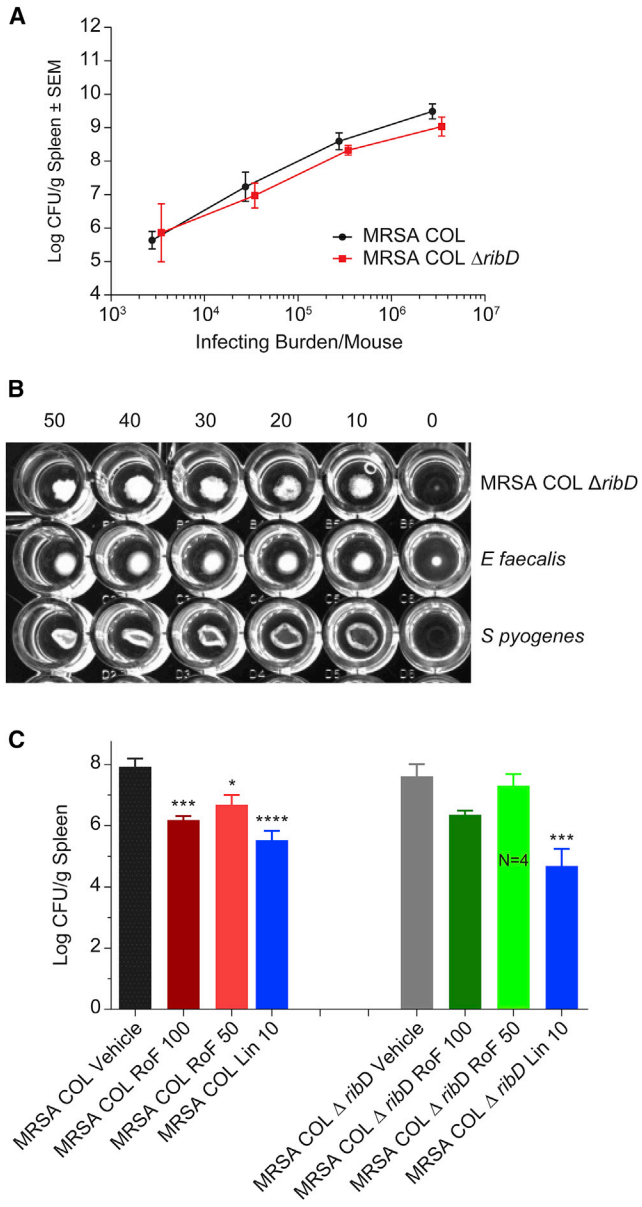

Figure 5. RoF Efficacy Requires Dual inhibition of *S. aureus* FMN Riboswitches

(A) Disruption of *S. aureus* RF de novo biosynthesis does not attenuate virulence in a murine septicemia model of infection. No difference in virulence was detected between MRSA COL parent (black) and the isogenic *ΔribD* strain (red) over a 3 $\log_{10}$ escalation in infectious dose examined. Mean spleen bacterial burden is graphed with error bars indicating SEM.

(B) RF auxotrophs MRSA COL *ΔribD*, *E. faecalis*, and *S. pyogenes* display robust growth in the presence of human serum. Bacterial growth was tested in low RF CAMH medium versus 10% serial increasing levels of heat-inactivated human serum (as labeled) provided as an exogenous source of RF.

(C) In vivo activity of RoF in a murine septicemia model of MRSA infection. Neutropenic BALB/c mice (5/group) were challenged by intraperitoneal injection with MRSA COL parent or Δ*ribD* mutant strain and treated with vehicle (10% DMSO), RoF (100 and 50 mg/kg) or the positive control antibiotic linezolid (Lin; 10 mg/kg). Spleens were aseptically collected from all surviving mice and the log(CFU per g spleen tissue) reduction by treatment was calculated on the basis of bacterial burden in spleens from the vehicle control group. All statistical analyses are performed by ANOVA (>3 groups compared). *$p < 0.05$ versus parent vehicle; ***$p < 0.001$ versus parent vehicle; ****$p < 0.0001$ versus parent vehicle; ***$p < 0.001$ versus *ΔribD* vehicle.

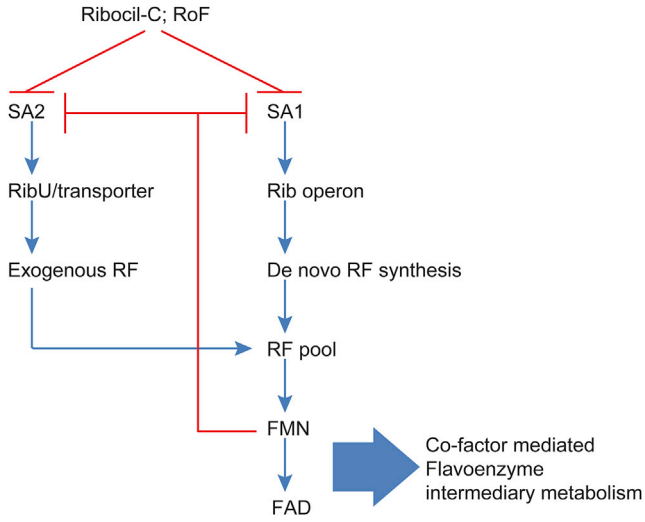

Figure 6. Targeting Dual FMN Riboswitches Uniquely Disrupts *S. aureus* RF Homeostasis

Dual-targeting small-molecule inhibitors of *S. aureus* SA1 and SA2 FMN riboswitches ensure simultaneous impairment of both RF de novo biosynthesis and RF uptake in an infectious setting. Such a dual mechanism of inhibition is required to consider RF homeostasis a suitable antibacterial drug target.

biosynthesis, and uptake in a host environment is predicted to display antibiotic efficacy in treating an MRSA infection.

DISCUSSION

Applying genetic, biophysical, computational, and cell biological methods we demonstrate ribocil-C and RoF both selectively inhibit two highly conserved but functionally distinct *S. aureus* FMN riboswitches coordinating RF biosynthesis and uptake, respectively. To our knowledge, this is the first time any antibacterial riboswitch inhibitor has been unequivocally demonstrated both in vitro as well as in a whole-cell context to target two independent riboswitches that mediate bacterial growth in a single bacterial pathogen. As we have recently demonstrated in *E. coli* (Howe et al., 2015), ribocil-C and RoF act as a synthetic mimic and antimetabolite of FMN, respectively, to disrupt FMN riboswitch-controlled gene expression and deplete FMN and FAD co-factors essential for *S. aureus* growth.

We predict that therapeutic efficacy of any antibacterial targeting GP RF metabolism must inhibit dual mechanisms of obtaining this essential vitamin; namely de novo RF synthesis as well as active uptake from the environment (Figure 6). Unlike GN bacteria, GP bacterial pathogens including *S. aureus*, *E. faecalis*, and *S. pyogenes* widely express highly efficient RF transporters. As such, they serve as endogenous drug resistance or "bypass" mechanisms potentially capable of suppressing the antibiotic effect of RF biosynthesis inhibitors. Indeed, this is likely the case as we demonstrate that natural RF levels in a murine infection model as well as in human serum contain sufficient RF to rescue growth and virulence of *S. aureus* rendered auxotrophic for RF

by genetic means. Moreover, RoF efficacy achieved in this same animal model demonstrates that FMN riboswitches which coordinate expression of RF biosynthesis and uptake pathways (rather than any of the individual enzymes required for RF biosynthesis or uptake) are uniquely validated as an antibacterial drug target in RF metabolism and for which cognate inhibitors are predicted to possess broad-spectrum efficacy. Performing such studies of conditionally essential genes under consideration as possible antibacterial targets early and in the context of an infectious setting is critically important to mitigate potential controversies over their drug target validation, as recently reported for *S. aureus* type II fatty acid biosynthesis (Brinster et al., 2009; Morvan et al., 2016).

Our studies exploit RoF and ribocil-C as chemical probes to consider new derivatives or entirely new chemical series of FMN riboswitch inhibitors serving as possible antibacterial agents to treat GP bacterial infections. As a chemical probe, RoF is a potent inhibitor with broad activity against *S. aureus* (including MRSA), *S. pyogenes*, and *E. faecalis.* Indeed, the superior potency of RoF versus ribocil-C is likely attributable to the active uptake of RoF rather than ribocil-C by GP bacteria. Perhaps surprising, RoF^R mutation analysis reveals RoF (and/or its ultimate conversion to RoFMN and RoFAD) to be highly selective in targeting each of the FMN riboswitches in *S. aureus* rather than obviously acting as a promiscuous inhibitor that competitively binds to FMN or FAD-requiring flavoenzymes, as reported in *E. coli* (Langer et al., 2013a; Langer el al. 2013b; Howe et al., 2015). This conclusion is based on our extensive genetic mapping of RoF^R mutations and identifying its primary drug target to be SA1 and SA2 FMN riboswitches; other mutations detected are exceedingly rare. Further, SA1 aptamer mutations conferring RoF^R provide a substantial shift in MIC (>512-fold), implying that, if RoF has a second distinct drug target, such as bacterial flavoenzyme(s), it is minor and does not substantially contribute to the antibacterial effect of RoF. We also conclude RoF is a more potent inhibitor of both SA1 and SA2 FMN riboswitches than ribocil-C since the RoF MIC is comparatively lower than ribocil-C against a wild-type MRSA strain in the absence of exogenous RF (a condition where SA1 riboswitch activity is specifically inhibited by the compound) as well as the isogenic Δ*ribD* mutant in the presence of RF (where SA2 riboswitch activity is specifically inhibited by the compound) (Tables 1 and S2).

The use of RoF as a chemical probe to interdict its drug target also reveals significant challenges which must be addressed by any antibacterial agent targeting FMN riboswitches. A central challenge is addressing the high resistance rate of *S. aureus* to RoF ($\sim 2 \times 10^{-7}$). Surprisingly, an analog of RoF (5FDQD) demonstrates potent *Clostridium difficile* antibacterial activity and displays an extremely low frequency of resistance ($<1 \times 10^{-9}$) to this agent (Blount et al., 2015). Whether chemical optimization of the RoF scaffold or an entirely new series such as ribocil-C with superior potency addresses this issue remains to be determined. Alternatively, RoF drug resistance may be mitigated in the context of a narrow-spectrum agent against natural RF auxotrophs, such as *E. faecalis*. For example, it is surprising that for *S. aureus* and *E. coli* (Howe et al., 2015), $drug^R$ mutations to RoF and ribocil-C almost completely map to their cognate target, the FMN riboswitch, whereas this does not similarly occur in *E. faecalis*. We speculate that this may reflect important structural or functional differences between *E. faecalis* and *S. aureus* or *E. coli* FMN riboswitches and that such difference(s) reflect a reduced tolerance to mutations that either constitutively induce *E. faecalis* expression of RibU or disrupt its expression; the latter of which would impair *E. faecalis* growth and would not be selected. Consistent with this view, the *E. faecalis* FMN riboswitch aptamer is smaller than its *S. aureus* SA2 counterpart and shares only 65% identity (Figure S8). We also note that the *E. faecalis* riboswitch expression platform is 2-fold larger than the *S. aureus* SA2 riboswitch expression platform and is predicted to adopt substantially greater secondary structure (Figure S8). Indeed, the FOR of RoF is much lower against *E. faecalis* ($\sim 2 \times 10^{-9}$) than *S. aureus*, consistent with the possible deleterious effects of such mutants within the riboswitch of a natural RF auxotroph. We speculate that in the case of *E. faecalis*, perhaps a combination of its "minimal" aptamer linked to an "expanded" expression platform reduces the likelihood of viable $drug^R$ aptamer mutations sufficient to maintain an "ON" conformation of the riboswitch. Finally, we note that RoF efficacy studies revealed signs of host toxicity, including lethargy and ruffled fur. As mammals lack the FMN riboswitch, perhaps this reflects off-target effects on host flavoenzymes.

In addition to the applied focus of this work, RoF^R studies highlight contextual differences in FMN riboswitch regulation of RF homeostasis among GP and GN bacteria. For example, SA1 RoF^R mutants in *S. aureus* constitutively express the RF biosynthetic pathway sufficient for survival (i.e., becoming "committed" prototrophs) while presumably repressing RibU-mediated active uptake of RoF. Consistent with such a transporter deficiency, a massive (>512-fold) resistance to RoF is observed in such mutants, paralleling the intrinsic RoF resistance of *E. coli*, which lack an RF transporter (Howe et al., 2015). Conversely, the *S. aureus* Δ*ribD* strain serves as a model RF auxotroph among GP bacteria, and SA2 RoF^R mutants in this background are implied to constitutively express RibU, reflecting an enhanced RF auxotrophy. Interestingly, such mutants display only a modest shift in RoF susceptibility (4- to 8-fold). Although such a phenotype is counterintuitive considering that in this context both RF and RoF would be more effectively transported into cells, we speculate more modest shifts in RoF susceptibility observed are a consequence of RF:RoF ratios. Whereas a low RF:RoF ratio favors RoFMN-mediated FMN riboswitch inhibition, a high RF:RoF suppresses the drug effect, and altered shifts in RoF MIC against these mutants is achieved by RF supplement levels (Table S2). As such, drug resistance to RoF and other FMN riboswitch inhibitors may be less significant among RF auxotrophs such as *S. pyogenes*, *E. faecalis*, and *Listeria* considering typical RF levels are low in a relevant infectious setting (Petteys and Frank, 2011) and consequently favor only a modest MIC shift among possible RoF^R isolates.

It is also intriguing that mutations mapping to the *S. aureus* FMN reductase Azo1 (Chen et al., 2005) confer profound resistance specifically to RoF. Perl and colleagues previously demonstrated that *B. subtilis* specifically synthesizes reduced forms of RF, FMN, and FAD (i.e., RF_{H2}, FMN_{H2}, and FAD_{H2}) and that only the reduced forms of each co-factor serve as substrate for the FAD flavokinase/synthetase (Kearney et al., 1979). The enzyme(s) responsible for converting RF, FMN, and FAD to their reduced form, however, remain unknown. We speculate that,

like *B. subtilis*, *S. aureus* may also utilize reduced forms of each co-factor and that Azo1 may functionally perform such a role. However, as Azo1 is not essential for *S. aureus* growth (Chaudhuri et al., 2009), oxidized forms of flavin co-factors must also be functionally active. Mechanistically, *S. aureus* RoF^R resistance may be achieved in a manner analogous to *B. subtilis ribC*820 mutants (Mack et al., 1998) such that *azo1* mutants may similarly reduce $FMN_{(H2)}$ levels sufficiently to induce FMN riboswitch-mediated overexpression of RF synthesis, thereby providing protection from RoF. Alternatively, Azo1 may directly reduce RoF to RoF_{H2} and provide a preferred substrate of the RibF flavokinase, yielding $RoFMN_{H2}$ and which may preferentially bind and inhibit the FMN riboswitch more effectively than FMN. In either instance, RoF^R *azo1* mutants may impair binding to the drug and/or ineffectively reduce RoF to its activated state. Indeed, recent studies in *B. subtilis* demonstrate that a RibR regulator protein with flavokinase activity specifically converts reduced RF (RFH_2) to $FMNH_2$ and that the latter is a more efficient effector of the FMN riboswitch than non-reduced FMN (Pedrolli et al., 2015b).

SIGNIFICANCE

An urgent need exists for new antibiotics with novel mechanisms of action to treat multi-drug-resistant bacteria. Riboswitches are bacterial-specific non-coding RNA structural elements that bind specific metabolites to regulate gene expression of metabolic pathways essential for growth. They are also absent from man. As such, they represent an unconventional and entirely unexploited class of potential antibacterial drug targets recently receiving significant interest since cognate inhibitors could ultimately serve as novel antibacterial agents. The FMN riboswitch regulates the biosynthesis and uptake of riboflavin (RF; vitamin B2) which is then converted to flavin mononucleotide (FMN) and flavin adenine dinucleotide (FAD); critical co-factors required by a variety of flavoenzymes and essential for bacterial growth. Two structurally distinct inhibitors of the FMN riboswitch have recently been reported. Ribocil-C and roseoflavin (RoF) are believed to mimic the endogenous riboswitch ligand, FMN, thereby repressing FMN riboswitch-regulated genes involved in RF homeostasis and ultimately depleting RF, FMN, and FAD levels. Here we demonstrate by genetic, biophysical, computational, biochemical, and pharmacological means that ribocil-C and RoF each selectively inhibits two separate FMN riboswitches controlling RF biosynthesis and uptake, respectively, in the Gram-positive drug-resistant bacterial pathogen, methicillin-resistant *Staphylococcus aureus* (MRSA). Having established their validity as dual-targeting FMN riboswitch inhibitors with whole-cell activity and selectivity, we utilize RoF as a chemical probe to evaluate the suitability of RF homeostasis as a valid antibiotic target pathway. We conclude that because *S. aureus* can acquire RF either by de novo synthesis or uptake from its environment (including in a host infection setting) FMN riboswitches serve as the sole target in RF homeostasis for which cognate inhibitors are predicted to have antibiotic efficacy in a murine infection model. We also discuss key antibiotic development challenges such inhibitors are likely to face in terms of antibiotic spectrum and propensity for resistance.

STAR★METHODS

Detailed methods are provided in the online version of this paper and include the following:

- KEY RESOURCES TABLE
- CONTACT FOR REAGENT AND RESOURCE SHARING
- EXPERIMENTAL MODEL AND SUBJECT DETAILS
  - In Vivo Animal Studies
- METHODS DETAILS
  - Microbiological Studies
  - Isolation of MRSA COL Roseoflavin (RoF) Resistant Mutants
  - Construction of MB5746 *pnuX*
  - Construction of MRSA COL Δ*ribD*
  - Virulence Studies
  - RoF Efficacy Studies in a Murine Systemic Infection Model
  - HPLC-Based Quantitative Analysis of Flavins
  - Fluorescence Detection of FMN Binding to SA Riboswitch Aptamers
  - Ribocil-C Steady State Competition Binding
  - Homology Modeling
  - Whole Genomic Sequencing and Bioinformatics Study
- QUANTIFICATION AND STATISTICAL ANALYSIS
- DATA AND SOFTWARE AVAILABILITY
  - Data Resources
  - Software

SUPPLEMENTAL INFORMATION

Supplemental Information includes eight figures and two tables and can be found with this article online at http://dx.doi.org/10.1016/j.chembiol.2017.03.014.

AUTHOR CONTRIBUTIONS

H.W., P.A.M., J.C.M., and M.D.M. performed genetic and microbiological experiments. A.V., T.M., and J.A.H. performed biochemical and biophysical experiments. N.M., C.M.B., L.X., and X.S. performed bioinformatics analyses. C.G., A.M.G., and A.F. performed animal studies. T.R. conceived the project and directed the research. H.W., M.M., and T.R. wrote the manuscript.

ACKNOWLEDGMENTS

We wish to thank Daria Hazuda for her unwavering support and commitment to basic research within Merck. We would also like to thank the reviewers for their thoughtful comments that helped strengthen the manuscript.

Received: December 6, 2016
Revised: February 3, 2017
Accepted: March 23, 2017
Published: April 20, 2017

REFERENCES

Baker, J.L., Sudarsan, N., Weinberg, Z., Roth, A., Stockbridge, R.B., and Breaker, R.R. (2012). Widespread genetic switches and toxicity resistance proteins for fluoride. Science *335*, 233–235.

Blount, K.F., and Breaker, R.R. (2006). Riboswitches as antibacterial drug targets. Nat. Biotechnol. *24*, 1558–1564.

Blount, K.F., Megyola, C., Plummer, M., Osterman, D., O'Connell, T., Aristoff, P., Quinn, C., Chrusciel, R.A., Poel, T.J., Schostarez, H.J., et al. (2015). Novel riboswitch-binding flavin analog that protects mice against *Clostridium difficile* infection without inhibiting cecal flora. Antimicrob. Agents Chemother. *59*, 5736–5746.

Breaker, R.R. (2011). Prospects for riboswitch discovery and analysis. Mol. Cell. *43*, 867–879.

Brinster, S., Lamberet, G., Staels, B., Trieu-Cuot, P., Gruss, A., and Poyart, C. (2009). Type II fatty acid synthesis is not a suitable antibiotic target for Gram-positive pathogens. Nature *458*, 83–86.

Burge, S.W., Daub, J., Eberhardt, R., Tate, J., Barquist, L., Nawrocki, E.P., Eddy, S.R., Gardner, P.P., and Bateman, A. (2012). Rfam 11.0: 10 years of RNA families. Nucleic Acids Res. *41*, D226–D232.

Chaudhuri, R.R., Allen, A.G., Owen, P.J., Shalom, G., Stone, K., Harrison, M., Burgis, T.A., Lockyer, M., Garcia-Lara, J., Foster, S.J., et al. (2009). Comprehensive identification of essential *Staphylococcus aureus* genes using Transposon-Mediated Differential Hybridisation (TMDH). BMC Genomics *10*, 291.

Chen, H., Hopper, S.L., and Cerniglia, C.E. (2005). Biochemical and molecular characterization of an azoreductase from *Staphylococcus aureus*, a tetrameric NADPH-dependent flavoprotein. Microbiology *151*, 1433–1441.

Fischer, M., and Bacher, A. (2005). Biosynthesis of flavocoenzymes. Nat. Prod. Rep. *22*, 324–350.

Gelfand, M.S., Mironov, A.A., Jomantas, J., Kozlov, Y.I., and Perumov, D.A. (1999). A conserved RNA structure element involved in the regulation of bacterial RF synthesis genes. Trends Genet. *15*, 439–442.

Gill, S.R., Fouts, D.E., Archer, G.L., Mongodin, E.F., Deboy, R.T., Ravel, J., Paulsen, I.T., Kolonay, J.F., Brinkac, L., Beanan, M., et al. (2005). Insights on evolution of virulence and resistance from the complete genome analysis of an early methicillin-resistant *Staphylococcus aureus* strain and a biofilm-producing methicillin-resistant *Staphylococcus epidermidis* strain. J. Bacteriol. *187*, 2426–2438.

Gutiérrez-Preciado, A., Torres, A.G., Merino, E., Bonomi, H.R., Goldbaum, F.A., and García-Angulo, V.A. (2015). Extensive identification of bacterial riboflavin transporters and their distribution across bacterial species. PLoS One *10*, e0126124.

Howe, J.A., Wang, H., Fischmann, T.O., Balibar, C.J., Xiao, L., Galgoci, A.M., Malinverni, J.C., Mayhood, T., Villafania, A., Nahvi, A., et al. (2015). Selective small-molecule inhibition of an RNA structural element. Nature *526*, 672–677.

Howe, J.A., Xiao, L., Fischmann, T.O., Wang, H., Tang, H., Villafania, A., Zhang, R., Barbieri, C.M., and Roemer, T. (2016). Atomic resolution mechanistic studies of ribocil: a highly selective unnatural ligand mimic of the *E. coli* FMN riboswitch. RNA Biol. *13*, 946–954.

Kearney, E.B., Goldenberg, J., Lipsick, J., and Perl, M. (1979). Flavokinase and FAD synthetase from *Bacillus subtilis* specific for reduced flavins. J. Biol. Chem. *254*, 9551–9557.

Kodali, S., Galgoci, A., Young, K., Painter, R., Silver, L.L., Herath, K.B., Singh, S.B., Cully, D., Barrett, J.F., Schmatz, D., and Wang, J. (2005). Determination of selectivity and efficacy of fatty acid synthesis inhibitors. J. Biol. Chem. *280*, 1669–1677.

Langer, S., Hashimoto, M., Hobl, B., Mathes, T., and Mack, M. (2013a). Flavoproteins are potential targets for the antibiotic roseoflavin in *Escherichia coli*. J. Bacteriol. *195*, 4037–4045.

Langer, S., Nakanishi, S., Mathes, T., Knaus, T., Binter, A., Macheroux, P., Mase, T., Miyakawa, T., Tanokura, M., and Mack, M. (2013b). The flavoenzyme azobenzene reductase AzoR from *Escherichia coli* binds roseoflavin mononucleotide (RoFMN) with high affinity and is less active in its RoFMN form. Biochemistry *52*, 4288–4295.

Lee, J.C. (1995). Electrotransformation of staphylococci. Methods Mol. Biol. *47*, 209–216.

Lee, E.R., Blount, K.F., and Breaker, R.R. (2009). Roseoflavin is a natural antibacterial compound that binds to FMN riboswitches and regulates gene expression. RNA Biol. *6*, 187–194.

Lee, S.H., Wang, H., Labroli, M., Koseoglu, S., Zuck, P., Mayhood, T., Gill, C., Mann, P., Sher, X., Ha, S., et al. (2016). TarO-specific inhibitors of wall teichoic acid biosynthesis restore β-lactam efficacy against methicillin-resistant staphylococci. Sci. Transl. Med. *8*, 329ra32.

Li, H., and Durbin, R. (2009). Fast and accurate short read alignment with Burrows-Wheeler Transform. Bioinformatics *25*, 1754–1760.

Lu, X.J., and Olson, W.K. (2003). 3DNA: a software package for the analysis, rebuilding and visualization of three-dimensional nucleic acid structures. Nucleic Acids Res. *31*, 5108–5121.

Lünse, C.E., Schüller, A., and Mayer, G. (2014). The promise of riboswitches as potential antibacterial drug targets. Int. J. Med. Microbiol. *304*, 79–92.

Mack, M., van Loon, A.P., and Hohmann, H.P. (1998). Regulation of RF biosynthesis in *Bacillus subtilis* is affected by the activity of the flavokinase/flavin adenine dinucleotide synthetase encoded by ribC. J. Bacteriol. *180*, 950–955.

Mann, P.A., Müller, A., Wolff, K.A., Fischmann, T., Wang, H., Reed, P., Hou, Y., Li, W., Müller, C.E., Xiao, J., et al. (2016). Chemical genetic analysis and functional characterization of staphylococcal wall teichoic acid 2-Epimerases reveals unconventional antibiotic drug targets. PLoS Pathog. *12*, e1005585.

Mansjö, M., and Johansson, J. (2011). The riboflavin analog roseoflavin targets an FMN-riboswitch and blocks *Listeria monocytogenes* growth, but also stimulates virulence gene-expression and infection. RNA Biol. *8*, 674–680.

Matzner, D., and Mayer, G. (2015). (Dis)similar analogues of riboswitch metabolites as antibacterial lead compounds. J. Med. Chem. *58*, 3275–3286.

McKenna, A., Hanna, M., Banks, E., Sivachenko, A., Cibulskis, K., Kernytsky, A., Garimella, K., Altshuler, D., Gabriel, S., Daly, M., and DePristo, M.A. (2010). The Genome Analysis Toolkit: a MapReduce framework for analyzing next-generation DNA sequencing data. Genome Res. *20*, 1297–1303.

Mellin, J.R., and Cossart, P. (2015). Unexpected versatility in bacterial riboswitches. Trends Genet. *31*, 150–156.

Mironov, A.S., Gusarov, I., Rafikov, R., Lopez, L.E., Shatalin, K., Kreneva, R.A., Perumov, D.A., and Nudler, E. (2002). Sensing small molecules by nascent RNA: a mechanism to control transcription in bacteria. Cell *111*, 747–756.

Morvan, C., Halpern, D., Kénanian, G., Hays, C., Anba-Mondoloni, J., Brinster, S., Kennedy, S., Trieu-Cuot, P., Poyart, C., Lamberet, G., et al. (2016). Environmental fatty acids enable emergence of infectious *Staphylococcus aureus* resistant to FASII-targeted antimicrobials. Nat. Commun. *7*, 12944.

Mulhbacher, J., Brouillette, E., Allard, M., Fortier, L.C., Malouin, F., and Lafontaine, D.A. (2010). Novel riboswitch ligand analogs as selective inhibitors of guanine-related metabolic pathways. PLoS Pathog. *6*, e1000865.

Nawrocki, E.P., Burge, S.W., Bateman, A., Daub, J., Eberhardt, R.Y., Eddy, S.R., Floden, E.W., Gardner, P.P., Jones, T.A., Tate, J., et al. (2015). Rfam 12.0: updates to the RNA families database. Nucleic Acids Res. *43*, D130–D137.

Otani, S., Takatsu, M., Nakano, M., Kasai, S., and Miura, R. (1974). Roseoflavin, a new antimicrobial pigment from *Streptomyces*. J. Antibiot. *27*, 86–87.

Ott, E., Stolz, J., Lehmann, M., and Mack, M. (2009). The RFN riboswitch of *Bacillus subtilis* is a target for the antibiotic roseoflavin produced by *Streptomyces davawensis*. RNA Biol. *6*, 276–280.

Pedrolli, D.B., Matern, A., Wang, J., Ester, M., Siedler, K., Breaker, R., and Mack, M. (2012). A highly specialized flavin mononucleotide riboswitch responds differently to similar ligands and confers roseoflavin resistance to *Streptomyces davawensis*. Nucleic Acids Res. *40*, 8662–8673.

Pedrolli, D.B., Jankowitsch, F., Schwarz, J., Langer, S., Nakanishi, S., Frei, E., and Mack, M. (2013). RF analogs as antiinfectives: occurrence, mode of action, metabolism and resistance. Curr. Pharm. Des. *19*, 2552–2560.

Pedrolli, D., Langer, S., Hobl, B., Schwarz, J., Hashimoto, M., and Mack, M. (2015a). The ribB FMN riboswitch from *Escherichia coli* operates at the transcriptional and translational level and regulates RF biosynthesis. FEBS J. *282*, 3230–3242.

Pedrolli, D.B., Kühm, C., Sévin, D.C., Vockenhuber, M.P., Sauer, U., Suess, B., and Mack, M. (2015b). A dual control mechanism synchronizes riboflavin and sulphur metabolism in *Bacillus subtilis*. Proc. Natl. Acad. Sci. USA *112*, 14054–14059.

Petteys, B.J., and Frank, E.L. (2011). Rapid determination of vitamin B_2; (riboflavin) in plasma by HPLC. Clin. Chim. Acta *412*, 38–43.

Serganov, A., and Nudler, E. (2013). A decade of riboswitches. Cell *152*, 17–24.

Serganov, A., Huang, L., and Patel, D.J. (2009). Coenzyme recognition and gene regulation by a flavin mononucleotide riboswitch. Nature *458*, 233–237.

Sudarsan, N., Cohen-Chalamish, S., Nakamura, S., Emilsson, G.M., and Breaker, R.R. (2005). Thiamine pyrophosphate riboswitches are targets for the antimicrobial compound pyrithiamine. Chem. Biol. *12*, 1325–1335.

Vitreschak, A.G., Rodionov, D.A., Mironov, A.A., and Gelfand, M.S. (2002). Regulation of RF biosynthesis and transport genes in bacteria by transcriptional and translational attenuation. Nucleic Acids Res. *30*, 3141–3151.

Vogl, C., Grill, S., Schilling, O., Stülke, J., Mack, M., and Stolz, J. (2007). Characterization of riboflavin (vitamin B2) transport proteins from *Bacillus subtilis* and *Corynebacterium glutamicum*. J. Bacteriol. *189*, 7367–7375.

Winkler, W.C., and Breaker, R.R. (2005). Regulation of bacterial gene expression by riboswitches. Annu. Rev. Microbiol. *59*, 487–517.

Winkler, W.C., Cohen-Chalamish, S., and Breaker, R.R. (2002). An mRNA structure that controls gene expression by binding FMN. Proc. Natl. Acad. Sci. USA *99*, 15908–15913.

Zhang, P., Wang, J., and Shi, Y. (2010). Structure and mechanism of the S component of a bacterial ECF transporter. Nature *468*, 717–720.

STAR★METHODS

KEY RESOURCES TABLE

REAGENT or RESOURCE	SOURCE	IDENTIFIER
Bacterial and Virus Strains		
Staphylococcus aureus, MRSA COL	Merck Collection, Gill et al., 2005	SACOL
Escherichia coli, antibiotic sensitized	Merck Collection, Kodali et al., 2005	MB5746
Corynebacterium glutamicum	ATCC, Vogl et al., 2007	ATCC13032
Streptococcus pyogenes	Merck Collection	CL10440
Enterococcus faecalis	Merck Collection	CLB21560
Chemicals, Peptides, and Recombinant Proteins		
Roseoflavin	MP Biomedicals	Cat# 02154252
Ribocils (A-C)	Merck Research	NA
Riboflavin	Sigma-Aldrich	PHR1054
Critical Commercial Assays		
Vitamin B2 HPLC detection kit and B2 column	ImmuChrom, GmbH	IC2300, IC2300rp
BigDye Terminator v3.1 Cycle Sequencing Kit	Applied Biosystems	4337455
Deposited Data		
E. faecalis CLB21560 genome, GenBank	This paper	Accn ID: CP019512
E. faecalis Resistor NGS, GenBank	This paper	Accn ID:SRP097739
S. aureus Resistor NGS, GenBank	This paper	Accn ID:SRP097757
S. aureus Resistor Sanger, GenBank	This paper	Accn ID:SRP098056
Experimental Models: Organisms/Strains		
DBA2 mice	Jackson Labs	000671
BALB/c mice	Jackson Labs	000651
Oligonucleotides		
1768, Fwd Seq Sa1 *ribB* aptamer: CAAGTGCTTGAACCTCCGCA	This paper	NA
1769, Rev Seq Sa1 *ribB* aptamer: GCAACAACAGCGCAGTGACAATCA	This paper	NA
1770, Fwd Seq Sa2 *ribU* aptamer: GCTAGTAGTGACGGTACATCA	This paper	NA
1771, Rev Seq Sa2 *ribU* aptamer: GACGATTTTTACTCAATTGAGTGAT	This paper	NA
1796, *S. aureus ribD* KO construction, Fwd primer with Pst1 site: CAGCAGCAGCTGCAGCATCATTTCGGCAATGCACCGCT	This paper	NA
1801, *S. aureus ribD* KO construction, Rev primer with Eco RV site: CAGCAGCAGGATATCTCTTGTCCTTTCGCCATCGTGCCA	This paper	NA
1804, internal reverse primer for *S. aureus ribD* deletion: ATTTCAATA TTTGTTTGATTGGTTGTTAAATTTGGTGCACCAATACCAACAATCCT	This paper	NA
1806, internal forward primer for *S. aureus ribD* deletion: GTAGTTAAA GAAGGTAGGATTGTTGGTATTGGTGCACCAAATTTAACAACCAATCAA	This paper	NA
1792, *C. glutamicum pnuX* cloning with Nde1 site, Fwd: GTGGTGGTG CATATGAATCCTATAACCGAATTATTA	This paper	NA
1793, *C. glutamicum pnuX* cloning with BamH1 site, Rev: GTGGTGGT GGGATCCTCAGACTGTCACAGACTCCTGAGCT	This paper	NA
1794, T7 promoter primer for pET29 inserts: TAATACGACTCACTATAG	EMD Millipore	Cat# 69,348
1795, T7 terminator primer for pET29 inserts: GCTAGTTATTGCTCAGCG	This paper	NA
1829, *S. aureus*, Azo1 FMN reductase Fwd seq: GTGGTGTTGGAAAAGCT	This paper	NA
1831, *S. aureus*, Azo1 FMN reductase Rev seq: GGCATGTGACTT AAAAGCATTCTCA	This paper	NA
1843, *E. faecalis*, *ribU* transporter Fwd seq: CCCTGCAGAAAAATAGGGT	This paper	NA
1845, *E. faecalis*, *ribU* transporter Rev seq: CAACCTCTTTTCTTTTAGGCGT	This paper	NA

(*Continued on next page*)

Continued

REAGENT or RESOURCE	SOURCE	IDENTIFIER
1920, *E. faecalis*, FAD binding enzyme(EF1586) Fwd seq: CGTAGTCG TAGGATGTACCCA	This paper	NA
1921, *E. faecalis*, FAD binding enzyme (EF1586) Rev seq: GCGGTCT AACCCGTCAACT	This paper	NA
1922, *E. faecalis*, intergnic (EF2734-2735) Fwd seq: CCAAGTGGC GGCATTCACT	This paper	NA
1923, *E. faecalis*, intergnic (EF2734-2735) Rev seq: GCTGTGCCAGAA TAGCCT	This paper	NA
Recombinant DNA		
pnuX from *C. glutamicum* cloned into pET29 using Nde1& BamH1	This paper	NA
ΔribD constructed from S. aureus using 2-way PCR and cloned into pSAKO^{ts}	This paper; vector from Mann et al., 2016	NA
Software and Algorithms		
Sequencher 5.0	Gene Codes	Version 5.0
Vector NTI Advance	Invitrogen	11.5.1
Prism 7.02	Graph Pad	graphpad.com/
program mutate_bases	3DNA	x3dna.org/
SeqPrep	https://github.com/jstjohn/SeqPrep	
BWA algorithm	Li and Durbin, 2009	biobwa.sourceforge.net/bwa.shtml
GATK (Genome Analysis Toolkit)	Broad Institute	software.broadinstitute.org/gatk/

CONTACT FOR REAGENT AND RESOURCE SHARING

Further information and requests for resources and reagents should be directed to the lead contact, Terry Roemer (terry_roemer@merck.com or troemer@prokaryotics.com)

EXPERIMENTAL MODEL AND SUBJECT DETAILS

In Vivo Animal Studies

Fourteen week old female DBA2 mice (Jackson Labs) were treated, i.p., with 150 mg/kg cyclophosphamide (Baxter, NDC# 10019-955-50) on Day -4 and 100 mg/kg on Day -1 for virulence study. Female Balb/c mice were rendered neutropenic with a single intraperitoneal dose of cyclophosphamide (250 mg/kg) on day −4 for RoF efficacy study. All animal procedures were performed according to the protocol reviewed and approved by the Institutional Animal Care and Use Committee of Merck and Co. Inc.

METHODS DETAILS

Microbiological Studies

MRSA COL is a hospital-acquired pathogen commonly used in *Staphylococcus aureus* studies and has a fully sequenced and annotated genome (Gill et al., 2005). Like other Gram-positive strains, it harbors riboflavin biosynthesis genes as well as RF-specific uptake transporters (Winkler et al., 2002). MB5746 is an antibiotic-sensitized *E. coli* strain (Kodali et al., 2005), and does not possess RF transporters (Pedrolli et al., 2015a, 2015b). *Streptococcus pyogenes* and *Enterococcus faecalis* are riboflavin auxotrophs and lack riboflavin biosynthetic enzymes (Gutiérrez-Preciado et al., 2015). Accordingly, cation-adjusted Mueller Hinton broth (CAMHB) (Difco) was used to grow MB5746 and MRSA COL. CAMHB supplemented with RF was used for MRSA COL Δ*ribD* and *E. faecalis* strain CLB21560. CAMHB supplemented with 5% lysed horse blood was used for *S. pyogenes strain* CL10440. MICs were determined by the broth microdilution method as recommended by the Clinical and Laboratory Standards Institute. The activity of compounds was also evaluated with CAMH agar containing $5X10^6$ CFU of corresponding test strains.

Isolation of MRSA COL Roseoflavin (RoF) Resistant Mutants

MRSA COL was grown to late-exponential phase (OD600 ~1.0; approximately $5X10^9$ CFU/ml) in CAMHB and 100 μl of this broth was spread on CAMH agar plates containing 2-fold escalating agar MIC levels of roseoflavin (RoF) (MP Biomed). To establish the number of viable cells in the starting inoculum, the culture was serially diluted and plated on CAMH agar plates. Resistant isolates were re-streaked on plates containing the same RoF concentration. In the case of MRSA COL Δ*ribD* deletion mutant, CAMHB and CAMH agar were supplemented with 12.5 nM RF.

Construction of MB5746 *pnuX*

Corynebacterium glutamicum ATCC13032 (Vogl et al., 2007) was grown overnight in 5 ml Trypticase Soy broth and genomic DNA was prepared using a QiaAmp Blood and Tissue Kit (Qiagen, Valencia, CA). The *pnuX* open reading frame was amplified from *C. glutamicum* using Phusion high-fidelity polymerase (New England Biolabs; Ipswich, MA) and primers *pnuX* Fwd (1792): 5'-GTGGTGGTG*CATATG*AATCCTATAACCGAATTATTA-3' and *pnuX* Rev (1793): 5'-GTGGTGGTG*GGATCC*TCAGACTGTCACA GACTCCTGAGCT-3'. The respective *NdeI* and *BamHI* sites within primers 1792 and 1793 are underlined. The amplified *pnuX* product and pET29a were digested with *NdeI* and *BamHI*, purified using QIAquick PCR purification kit (Qiagen, Valencia, CA), and subsequently ligated using T4 DNA ligase (New England Biolabs; Ipswich, MA). The ligation reaction was transformed into electrocompetent MB5746 *E. coli* cells according to standard protocol (Bio-Rad MicroPulser; Hercules, CA), and transformants were selected on Luria-Bertani supplemented with Kanamycin at 50 μg/ml. The desired clone was confirmed by sequencing the insert using T7 promoter and terminator primers.

Construction of MRSA COL Δ*ribD*

Suicide plasmid pSAKO^{TS} (Mann et al., 2016) was used to construct an unmarked, in-frame deletion of the *ribD* biosynthetic gene. Amino acid residues 51 through 250 were targeted for deletion using two-way PCR. Approximately 1.2 kB of *ribD* upstream and 0.15 kB of N-term coding sequence was PCR amplified from MRSA COL with primers 1796 and 1804, appending a Pst1 restriction site. Similarly, sequence corresponding to AA residues 251 to the end of the *ribD* coding region and 1.2kB beyond was amplified with primers 1801 and 1806, appending a EcoRV restriction site. To create overlap with the first PCR fragment, 36 nucleotides corresponding to AA residues 39 through 50, were added to the 5' end of primer 1806. The two overlapping fragments were stitched together with ExTaq polymerase (Takara Clontech) using primers 1796 + 1801, restriction digested with *Pst1* and *EcoRV* (New England Biolabs), then cloned into pSAKO^{TS}. This deletion plasmid was used to electrotransform Methicillin sensitive *Staphylococcus aureus* RN4220 to Kanamycin (Kan) resistance, selected at the permissive 30°C temperature (Lee, 1995). Kan resistant colonies that were also sucrose sensitive were confirmed by PCR to harbor the deletion plasmid. To integrate the plasmid at the *ribD* locus, a single RN4220 transformant was inoculated into 2 mL Cation Adjusted Mueller Hinton (CAMH) Broth (Difco) and grown for 2 hours at 30°C, then shifted to 42°C for 6 hours, then plated on CAMH Agar + Kan 20 μg ml^{-1}. Stable merodiploids demonstrating both the wild-type and *ΔribD* form by PCR, were recovered from the plates following overnight incubation at 42°C. A single merodiploid was used as a donor to transduce the *ribD/ΔribD/Kan^{R}* region into *S. aureus* COL using phage 80, selecting on CAMH Agar + Kan 20 μg ml^{-1}. To resolve to the haploid *ΔribD* or haploid WT form through counter selection of the *sacB* gene in the plasmid, a single Kan resistant, sucrose sensitive COL transductant was streaked onto Trypticase Soy (TS) Agar (Difco) plates containing 7.5% sucrose and incubating at 37°C for 48 hours. Twenty single colonies were picked from this plate and inoculated into 2 mL TS broth and grown overnight. Two of the twenty isolates grew poorly and were presumed to be *ΔribD* riboflavin auxotrophs. Resolved deletion and WT forms were confirmed by PCR using primers 1796+1801. The following oligonucleotides were used in this study:

Primer	Sequence	Description
1768	CAAGTGCTTGAACCTCCGCA	Forward sequencing primer, Sa1 *ribB* aptamer
1769	GCAACAACAGCGCAGTGACAATCA	Reverse sequencing primer, Sa1 *ribB* aptamer
1770	GCTAGTAGTGACGGTACATCA	Forward sequencing primer, Sa2 *ribU* aptamer
1771	GACGATTTTTACTCAATTGAGTGAT	Reverse sequencing primer, Sa2 *ribU* aptamer
1796	CAGCAGCAGCTGCAGCATCATTTCGGCAATGCACCGCT	*S. aureus ribD* KO (SACOL1820), forward with Pst1 site
1801	CAGCAGCAGGATATCTCTTGTCCTTTCGCCATCGTGCCA	*S. aureus ribD* KO, reverse with EcoRV site
1804	ATTTCAATATTTGTTTGATTGGTTGTTAAATTTGGTGCACC AATACCAACAATCCT	internal reverse primer for in-frame *ribD* deletion
1806	GTAGTTAAAGAAGGTAGGATTGTTGGTATTGGTGCACC AAATTTAACAACCAATCAA	internal forward primer for in-frame *ribD* deletion
1792	GTGGTGGTGCATATGAATCCTATAACCGAATTATTA	*pnuX* from *C. glutamicum* ATCC13032 cloning with Nde1 site
1793	GTGGTGGTGGGATCCTCAGACTGTCACAGACTCCTGAGCT	*pnuX* from *C. glutamicum* ATCC13032 cloning with BamH1 site
1794	TAATACGACTCACTATAG	T7 promoter primer for sequencing pET29 inserts
1795	GCTAGTTATTGCTCAGCG	T7 terminator primer for sequencing pET29 inserts
1829	GTGGTGTTGGAAAAGCT	Forward sequencing primer, SACOL, Azo1 FMN reductase
1831	GGCATGTGACTTAAAAGCATTCTCA	Reverse sequencing primer, SACOL, Azo1 FMN reductase
1843	CCCTGCAGAAAAATAGGGT	Forward sequencing primer, E. fs, *ribU* transporter
1845	CAACCTCTTTTCTTTTAGGCGT	Reverse sequencing primer, E. fs, *ribU* transporter
1920	CGTAGTCGTAGGATGTACCCA	Forward sequencing primer, E. fs, FAD binding enzyme (EF1586)
1921	GCGGTCTAACCCGTCAACT	Reverse sequencing primer, E. fs, FAD binding enzyme (EF1586)
1922	CCAAGTGGCGGCATTCACT	Forward sequencing primer, E. fs, intergnic (EF2734-2735)
1923	GCTGTGCCAGAATAGCCT	Reverse sequencing primer, E. fs, intergnic (EF2734-2735)

Virulence Studies

MRSA COL was pre-grown in 10 ml Trypticase Soy Broth (TSB, Corning, Cat# 46-060-CI); the isogenic MRSA COL Δ*ribD* deletion mutant was pre-grown in TSB supplemented with 230 nM riboflavin (Sigma, Cat#R4500-100G). Both strains were pre-grown at 35°C for 6 hr with shaking at 250 rpm. The respective 6 hr cultures were used to seed, 1 mL:50 mL, TSB either with or without 230 nM riboflavin in a 250 ml flask and were incubated at 35°C for 16 hours with shaking at 250 rpm. Overnight cultures were centrifuged at 5000 rpm for 12 minutes at 5°C. Supernatant was decanted and pellets were re-suspended in 50 mL fresh TSB to remove excess riboflavin. Six tenfold serial dilutions were made in TSB from these cultures ($5.5x10^9$ CFU/mL for MRSA COL, $6.9x10^9$ CFU/mL for Δ*ribD* strain). Select serial dilutions were further diluted 1:10 into 1% gastric hog mucin for intra-peritoneal (i.p.) injection into mice. The initial dilutions without mucin were plated for quantification on Brain Heart Infusion (BHI) agar plates. Fourteen week old female DBA2 mice (Jackson Labs) were treated, i.p., with 150 mg/kg cyclophosphamide (Baxter, NDC# 10019-955-50) on Day -4 and 100 mg/kg on Day -1. On Day 0, 5 mice per group were injected, i.p., 0.5 mL, with a respective dilution of bacterial stock in 1% mucin ($2.75x10^6$, 10^5, 10^4, 10^3 CFU/mL for COL, $3.45x10^6$, 10^5, 10^4, 10^3 CFU/mL for Δ*ribD*). On Day 1, subjects were euthanized via CO_2 asphyxiation and spleens were aseptically removed, weighed and homogenized in 1.5 mL of sterile saline (Hyclone, Cat# SH30028.03) with 10% glycerol (Fisher Scientific, Cat# BP229-1). Tissue homogenates were serially diluted tenfold in sterile saline and selected concentrations were plated on BHI agar plates. Plates were incubated at 35°C for 24 hours and colony forming units (CFU)/gram of spleen tissue were determined.

RoF Efficacy Studies in a Murine Systemic Infection Model

Female Balb/c mice were rendered neutropenic with a single intraperitoneal dose of cyclophosphamide (250 mg/kg) on day −4. MRSA COL parent and Δ*ribD* strain were grown for 16 hours in nutrient broth at 37°C, and 0.5 ml of diluted culture (~1×10^4 CFU) was administered intraperitoneally. RoF or vehicle was administered at 2, 5, and 8 hours after challenge, subcutaneously, three times a day. Twenty-four hours after challenge, the mice were euthanized, kidneys and spleens were harvested, weighed, homogenized, and plated to determine the CFUs remaining in the compound-treated groups as compared to the vehicle groups. Statistical analyses were determined using one-way ANOVA. All animal procedures were performed according to the protocol reviewed and approved by the Institutional Animal Care and Use Committee of Merck and Co. Inc.

HPLC-Based Quantitative Analysis of Flavins

Overnight cultures of MRSA COL and RoF resistant mutants were diluted 1:50 (≈4x10-7 CFU/ml) in CAMHB and distributed (1.25 ml) in 10 ml culture tubes containing diluted ribocil-C or RoF (2-fold dilution series) or DMSO (1%) as mock control. The treated cultures were incubated with shaking at 37°C for 20 hours after which the OD_{600} of the culture was determined and 500 μl was moved to a 96-well deep well plate. After centrifugation (4000 rpm) for 10 minutes the bacterial cell pellets were rinsed with PBS and centrifuged again. Cell pellets were then resuspended in 100ul of lysozyme solution [20 mM Tris HCL pH=8.0, 2 mM EDTA, 1.2% Triton X-100] with lysostaphin (3 μl of 10 mg /ml stock), incubated at 37°C for 30 minutes, and then frozen at -20°C. FMN and FAD concentrations in the bacterial lysates were determined using the Vitamin B2 HPLC detection kit (ImmuChrom, GmbH) and Vitamin B2 column (IC2300rp, ImmuChrom GmbH) following the procedure recommended by the manufacturer scaled for a 50 μl sample (bacterial lysate). A Shimadzu HPLC system with fluorescence detector was used at a flow rate of 1.0ml/min and flavin detection was carried out at 450 nm.

Fluorescence Detection of FMN Binding to SA Riboswitch Aptamers

FMN binding to the SA1 and SA2 riboswitch aptamers was monitored using the FMN fluorescence method described previously (Howe et al., 2015). Briefly, aptamers were reannealed at a 20-μM concentration in 4 mM KH_2PO_4, 16 mM K_2HPO_4, 64 mM KCl and 0.1 mM EDTA, pH 7.4 by heating at 95°C for 5 min followed by incubation at room temperature for 15 min. Solutions of various concentrations of each riboswitch were prepared in fluorescence assay buffer (50 mM Tris buffer, 100 mM KCl and 2 mM $MgCl_2$, pH 7.4) and incubated with 30, 60, and 120nM FMN for 2 hr after which fluorescence intensity was monitored using a Spectramax M5 (Molecular Devices, Sunnyvale, CA) at an excitation wavelength of 455 nm and emission wavelength at 525 nm with cutoff filter at 515 nm. The steady-state dissociation constant, K_d^{FMN}, was determined using the equation below.

$$I_{obs} = I_0 + \frac{I_\infty - I_0}{2FMN_t}\left(\left((RNA_t \times C_f) + FMN_t + K_d^{FMN}\right) - \sqrt{\left((RNA_t \times C_f) + FMN_t + K_d^{FMN}\right)^2 - 4(RNA_t \times C_f)FMN_t}\right)$$

I_{obs}, I_0, and I_∞ are the observed fluorescence signal, the fluorescence signal of unbound FMN, and the fluorescence signal of fully riboswitch-bound FMN, respectively. FMN_t and RNA_t are the total concentrations of FMN and riboswitch, respectively, at each data point. C_f is a correction factor applied to the RNA_t value to enable determination of the FMN-binding competent fraction of the total riboswitch RNA in the solution.

Ribocil-C Steady State Competition Binding

Ribocil-C binding to the SA1 and SA2 riboswitch aptamers was monitored using the FMN competition method previously described (Howe et al., 2015). In this study FMN and riboswitch aptamer concentrations were fixed at 60 and 150 nM, respectively, with various

concentrations of ribocil-C in fluorescence assay buffer containing 2 % DMSO. Following 2-hr incubation the FMN fluorescence signal was measured and the steady-state dissociation constant, $K_d^{ribocil}$, was determined using the set of equations below.

$$RNA_f = \frac{-A + 2\sqrt{(A^2 - 3B)}}{3} cos\left(\frac{arccos\left(\frac{(-2A^3 + 9AB - 27C)}{2\sqrt{(A^2-3B)^3}}\right)}{3}\right)$$

$$I_{obs} = FMN_t\left(I_0 + \frac{(I_\infty - I_0)RNA_f}{K_d^{FMN} + RNA_f}\right)$$

Where,

$$A = K_d^{FMN} + K_d^{ribocil} + FMN_t + ribocil_t - RNA_t \times C_f$$

$$B = K_d^{ribocil}(FMN_t - RNA_t \times C_f) + K_d^{FMN}(ribocil_t - RNA_t \times C_f) + K_d^{FMN}K_d^{ribocil}$$

$$C = -K_d^{FMN}K_d^{ribocil}RNA_t \times C_f$$

In these equations, I_{obs}, I_0, I_∞, FMN_t, C_f, and RNA_t are as defined above, while A, B, and C are the coefficients of the cubic solution to the explicit function defining RNA_f, which is the concentration of riboswitch aptamer not bound to FMN.

Homology Modeling

The homology models of both S. aureus SA1 and SA2 FMN aptamers were constructed using program mutate_bases (Lu and Olson, 2003) of the 3DNA package, with the *F. nucleatum* riboswitch aptamer X-ray structure as the template. The nucleotide sequence alignment was taken from Rfam database (Nawrocki et al., 2015). There are 34 and 31 base changes in SA1 and SA2 models, respectively, among the 111 nucleotides modeled. The ligands were modeled in the ligand binding site of SA1 and SA2 FMN aptamers through superimposing the homology models and the X-ray structures.

Whole Genomic Sequencing and Bioinformatics Study

All genomic DNA was prepared using the DNA Blood and Tissue Kit 69504 (Qiagen, Hilden, Germany) following the manufacturer's protocol. DNA was sequenced by the vendor (Expression Analysis, Morrisville, NC) using 150bp paired-end (PE) Illumina sequence reads with minimum 150X genome coverage. Sequence reads were cleaned with SeqPrep (https://github.com/jstjohn/SeqPrep) before aligning to the reference genome of *S. aureus* strain COL (NC_002951.2) using BWA algorithm (Li and Durbin, 2009), followed by variant calling using GATK (Genome Analysis Toolkit) (McKenna et al., 2010). Minimum 20X reads coverage on the variant loci and 75% variant reads frequency are required for the final variant calls. Variants were annotated using an in-house variant annotation script. In parallel, we performed Sanger-based sequencing on riboswitches and riboflavin coding regions using the BigDye Terminator v3.1 Cycle Sequencing Kit 4337455 (Applied Biosystems, Thermo Fisher Scientific, Waltham, MA) following the manufacturer's protocol. Sequences were deposited in GenBank with the following accession numbers:

Item	GenBank Accession(s)	number of Sequences	GenBank Submission ID	Bioproject ID
E. faecalis CLB21560 Genome	CP019512	3	SUB2356182	PRJNA368724
E. faecalis Resistor NGS	SRP097739	4	SUB2338895	PRJNA368646
S. aureus Resistor NGS	SRP097757	26	SUB2351500	PRJNA368710
S. aureus Resistor Sanger	SRP098056	59	SUB2356743	PRJNA369051

QUANTIFICATION AND STATISTICAL ANALYSIS

All data fitting and statistical analysis were performed using GraphPad Prism version 7.02, GraphPad Software, La Jolla California USA, www.graphpad.com. Statistical values and statistical significance were also reported in the related figure or figure legends. Statistical significance was defined as $p < 0.05$ and determined by one-way ANOVA.

DATA AND SOFTWARE AVAILABILITY

Data Resources

The DNA sequencing data reported in this paper has been deposited in GenBank under the accession number of CP019512, SRP097739, SRP097757, and SRP098056.

Software

All software used in this study was listed in the Key Resources Table and described in the detailed methods where applicable.